

VŠB – Technical University of Ostrava
Faculty of Electrical Engineering and Computer Science
Department of Cybernetics and Biomedical Engineering

Optimum Localization of Phonocardiographic Sensors and Analysis of These Signals

Optimalizace umístění fonokardiografického senzoru a analýza měřených signálů

Diploma Thesis Assignment

Student:

Bc. Karel Fojtík

Study Programme:

N2649 Electrical Engineering

Study Branch:

3901T009 Biomedical Engineering

Title:

Optimum Localization of Phonocardiographic Sensors and Analysis
of These Signals
Optimalizace umístění fonokardiografického senzoru a analýza
měřených signálů

The thesis language:

English

Description:

1. Bibliographic study.
2. Records of multiple (Phonocardiography)PCG signals in various degraded situations and analysis of these signals.
3. Implementation and testing of existing methods.
4. Design, implementation and testion of own method for PCG signal analysis.
5. Estimation of heart rate from measured PCG signals.
6. Evaluation of results.

References:

- [1] PAN, Sinno Jialin and Qiang YANG. A Survey on Transfer Learning. *IEEE Transactions on Knowledge and Data Engineering*, 2010. Vol. 22, iss. 10, pp. 1345-1359. Print ISSN 1041-4347. DOI: 10.1109/TKDE.2009.191.
- [2] TORREY, Lisa and Jude SHAVLIK. Transfer Learning. In E. Soria, J. Martin, R. Magdalena, M. Martinez and A. Serrano, editors, *Handbook of Research on Machine Learning Applications*, IGI Global 2009. pp. 242-264. ISBN 1605667676.

Extent and terms of a thesis are specified in directions for its elaboration that are opened to the public on the web sites of the faculty.

Supervisor:

doc. Ing. Martin Černý, Ph.D.

Date of issue: 01.09.2017

Date of submission: 30.04.2019



doc. Ing. Jiří Koziolek, Ph.D.
Head of Department



prof. Ing. Pavel Brandštetter, CSc.
Dean

I hereby declare that this master's thesis was written by myself. I have quoted all the references
I have drawn upon.

Ostrava, 30 April 2019



.....

I would like to thank doc. Ing. Martin Černý, Ph.D. for mentoring of this work, Julie Fontecave - Jallon for supervision during the internship and also Ing. Martina Litschmannová, Ph.D. for her help with the statistics.

Abstrakt

Tato práce je zaměřená na měření srdečních ozev, umístění senzorů srdečních ozev a následnou analýzu získaných signálů. V rámci této práce byly navrženy dvě auskultační sítě, pro synchronizované měření několika PCG signálů najednou. Rovněž byl navrhnutý automatický multikanálový detektor první a druhé srdeční ozvy. Navržený detektor využívá Shannonovy energie k získání obálky fonokardiografického signálu a následnou synchronizaci s R hrotem a T vlnou elektrokardiogramu k přesnému určení srdečních ozev. Hlavním výsledkem této práce je analýza fonokardiografického signálu získaného z jednotlivých míst na hrudníku a porovnání rozdílů pro různá auskultační místa v časové oblasti.

Klíčová slova: Fonokardiografie; PCG; Auskultace; Auskultační síť; Lokalizace; Zpracování signálu

Abstract

This work is focused on measurement of heart sounds, localization of PCG sensors and analysis of the acquired signals. Two auscultation sites were designed for the synchronized measurement of several PCG signals. The automatic multiple source heart sound detector of the first and the second heart sound was designed as well. The designed detector uses the Shannon energy to obtain an envelope of a PCG signal and synchronization with the R peak and the T wave of an electrocardiogram for accurate determination of the heart sounds. The main result of this work is the analysis of the phonocardiographic signal obtained from different positions on the chest and the comparison of the differences in the time domain for various auscultation areas.

Key Words: Phonocardiography; PCG; Auscultation; Auscultation site; Localisation; Signal Processing

Contents

List of symbols and abbreviations	13
List of Figures	15
List of Tables	17
Introduction	21
1 PCG Signal	23
1.1 Cardiac Cycle	23
1.2 Heart Sounds	28
1.3 Heart Murmurs	30
1.4 Auscultation	32
1.5 Electrocardiography	33
1.6 Phonocardiography	35
1.7 Used Equipment	37
1.8 Software	38
2 Data Acquisition	39
2.1 Auscultation Site A	39
2.2 Auscultation Site B	41
2.3 ECG Measuring	41
2.4 Measurement Protocol	42
2.5 Measuring of Damaged data	43
3 Heart Sound Detection	45
3.1 Existing Methods for Detecting Heart Sounds	45
3.2 Heart Sound Detector Realization	46
3.3 PCG Preprocessing	46
3.4 ECG Processing	52
4 Analysis of the Heart Sounds	59
4.1 R - R and S1 - S1 interval analysis	59
4.2 Testing between Measurements	72
4.3 R - S1 Interval Analysis	74
4.4 R - S2 Interval Analysis	86
Conclusion	99

References	101
Appendix	107

List of symbols and abbreviations

WHO	– World Health Organization
CVDs	– Cardiovascular Diseases
PCG	– Phonocardiography
ECG	– Electrocardiography
S1	– First Heart Sound
S2	– Second Heart Sound

List of Figures

1	Isovolumetric Contraction	24
2	Ventricular Ejection	25
3	Isovolumetric Relaxation	25
4	Rapid Ventricular Filling	26
5	Atrial Contraction	27
6	Cardiac Cycle	28
7	Murmurs Overview	31
8	Auscultation Areas	33
9	Electrical Conduction System	34
10	Auscultation Site A	39
11	Measuring Using Auscultation Site A	40
12	Auscultation Site B	41
13	ECG - Limb Leads	42
14	Different Types of Attachment	43
15	Heart Sound Detector - Block Diagram	46
16	PCG Preprocessing - Block Diagram	47
17	PCG Filtration	47
18	PCG Normalization	48
19	PCG Segmentation	49
20	Comparison Between Different Envelope Methods	49
21	Comparison of Calculated Envelops Using Different Order	51
22	PCG - Envelope Filtration	52
23	ECG - R Peak Detection - Block Diagram	52
24	ECG Processing	54
25	Heart Sound Detection - Block Diagram	54
26	Different Ways Obtaining S1s and S2s	56
27	Examined Intervals	57
28	R - R and S1 - S1 Interval	60
29	Duration of S1 - S1 (R - R) interval	62
30	Duration of S1 - S1 (R - R) interval	68
31	R - S1 Intervals	74
32	Auscultation site A, Patient A: Duration of R - S1 interval (ms)	75
33	Auscultation site B, Patient A: Duration of R - S1 interval (ms)	83
34	R - S2 Intervals	86
35	Auscultation Site A, Patient A: Duration of R - S2 interval (ms)	87
36	Auscultation Site B, Patient A: Duration of R - S2 interval (ms)	95

List of Tables

1	Technical Parameters of PowerLab 16/35	37
2	Technical Parameters of Microphone MLT201	38
3	Explanatory Notes to the Auscultation Site	40
4	Measuring Protocol for Damaged Data	43
5	Computation of the Intervals	57
6	Auscultation Site A, Patient A: Duration of S1 - S1 (R - R) interval (ms)	61
7	Auscultation Site A, Patient A: Confidence Intervals for Median of S1 - S1 Interval (ms)	63
8	Auscultation Site A, Patient A: Confidence Intervals for Median of S1 Abs - S1 Abs Interval (ms)	63
9	Auscultation Site A, Patient B: Confidence Intervals for Median of S1 - S1 Interval (ms)	64
10	Auscultation Site A, Patient B: Confidence Intervals for Median of S1 Abs - S1 Abs Interval (ms)	64
11	Friedman Test: P - values	65
12	Auscultation Site A, Patient A: Paired Samples Wilcoxon Test: p - values	66
13	Auscultation Site A, Patient B: Paired Samples Wilcoxon Test: p - values	67
14	Auscultation Site B: Duration of S1 - S1 (R - R) Interval (ms)	68
15	Auscultation Site B, Patient A: Confidence Intervals for Median of S1 - S1 Interval (ms)	69
16	Auscultation Site B, Patient A: Confidence Intervals for Median of S1 Abs - S1 Abs Interval (ms)	69
17	Auscultation Site B, Patient B: Confidence Intervals for Median of S1 - S1 Interval (ms)	70
18	Auscultation Site B, Patient B: Confidence Intervals for Median of S1 Abs - S1 Abs Interval (ms)	70
19	Friedman Test: P - values	71
20	Auscultation Site B, Patient A: Paired Samples Wilcoxon Test: p - values	72
21	Auscultation Site B, Patient B: Paired Samples Wilcoxon Test: p - values	72
22	Auscultation Site A, Patient A: Duration of R - S1 interval (ms)	76
23	Auscultation Site A, Patient A: Confidence Intervals for Median of R - S1 Interval (ms)	77
24	Auscultation Site A, Patient A: Confidence Intervals for Median of R - S1 Abs Interval (ms)	78
25	Auscultation Site A, Patient B: Confidence Intervals for Median of R - S1 Interval (ms)	78

26	Auscultation Site A, Patient B: Confidence Intervals for Median of R - S1 Abs Interval (ms)	79
27	Friedman test: P - values	80
28	Auscultation Site A, Patient A, R - S1 Interval: P - Values from Post Hoc Analysis	80
29	Auscultation Site A, Patient A, R - S1 Abs Interval: P - Values from Post Hoc Analysis	81
30	Auscultation Site A, Patient B, R - S1 Interval: P - Values from Post Hoc Analysis	81
31	Auscultation Site A, Patient B, R - S1 Abs Interval: P - Values from Post Hoc Analysis	81
32	Auscultation Site B, Patient A: Duration of R - S1 interval (ms)	82
33	Auscultation Site B, Patient A: Confidence Intervals for Median of R - S1 Interval (ms)	84
34	Auscultation Site B, Patient A: Confidence Intervals for Median of R - S1 Abs Interval (ms)	84
35	Auscultation Site B, Patient B: Confidence Intervals for Median of R - S1 Interval (ms)	84
36	Auscultation Site B, Patient B: Confidence Intervals for Median of R - S1 Abs Interval (ms)	84
37	Friedman Test: P - values	85
38	Auscultation Site A, Patient A: Duration of R - S2 Interval (ms)	88
39	Auscultation Site A, Patient A: Confidence Intervals for Median of R - S2 Interval (ms)	89
40	Auscultation Site A, Patient A: Confidence Intervals for Median of R - S2 Abs Interval (ms)	90
41	Auscultation Site A, Patient B: Confidence Intervals for Median of R - S2 Interval (ms)	90
42	Auscultation Site A, Patient B: Confidence Intervals for Median of R - S2 Abs Interval (ms)	91
43	Friedman Test: P - values	92
44	Patient A, R - S2 interval: P - Values from Post Hoc Analysis	92
45	Patient A, R - S2 Abs interval: P - Values from Post Hoc Analysis	93
46	Patient B, R - S2 interval: P - Values from Post Hoc Analysis	93
47	Patient B, R - S2 Abs interval: P - Values from Post Hoc Analysis	94
48	Auscultation Site B, Patient A: Duration of R - S2 interval (ms)	95
49	Auscultation Site B, Patient A: Confidence Intervals for Median of R - S2 Interval (ms)	96
50	Auscultation Site B, Patient A: Confidence Intervals for Median of R - S2 Abs Interval (ms)	96

51	Auscultation Site B, Patient B: Confidence Intervals for Median of R - S2 Interval (ms)	96
52	Auscultation Site B, Patient B: Confidence Intervals for Median of R - S2 Abs Interval (ms)	97
53	Friedman test: p - values	97
54	Patient A, Auscultation site B, R - S2 Abs interval: P - Values from Post Hoc Analysis	98
55	Patient B, Auscultation site B, R - S2 interval: P - Values from Post Hoc Analysis	98

Introduction

Due to WHO report from 2015 [9] cardiovascular diseases continue to be the leading cause of morbidity and mortality worldwide. One of the first steps in evaluating the cardiovascular system in clinical practice is a physical examination. Heart auscultation it is the essential and one of the most useful medical diagnostic tools for getting valuable information concerning the function of the heart valves and hemodynamics of the heart and may reveal many pathological cardiac conditions such as arrhythmias, valve disease, heart failure and more. Heart sounds provide important initial clues in disease evaluation, serve as a guide for a further diagnostic examination and thus play an important role in the early detection for CVDs. That is the reason why is a stethoscope often the first screening tool utilized by primary care providers. [1, 3, 4]

However, quality of the examination using traditional stethoscope is inconsistent, subjective and dependent on experience of an examiner. Highly trained personnel can provide more accurate information but they are still limited by human ear possibilities which is poorly suited for cardiac auscultation. The heart sound signal has much more information than can be assessed by traditional auscultation, therefore, phonocardiography was developed (PCG). Since the recordings from phonocardiograph can be processed through a computer many new possibilities for analysis of the measured signal were acquired. The analysed data can obtain both qualitative and quantitative characteristics of the phonocardiogram (PCG) signals and provide many pieces of information in both time and frequency spectrum. Concurrently with development of computer-aided auscultation, the algorithms can automatically detect even inaudible sounds and very precisely recognize pathological phenomena.[12, 15, 16, 19]

Unlike ECG there is no standardization in PCG and even if new methods of detection features are still coming there is no common way how to measure PCG data and practically no recent research in this area. An important factor for data acquisition is placement of sensors (microphone), type of sensors (technical parameters of sensor) and the way of attaching them to the human body.

The first part of the thesis deals with theoretical background of the human heart anatomy and function and genesis of PCG signal. The next part describes data acquisition and the used auscultation sites. The following part is focused on signal processing and describes the algorithm for detection of S1 and S2 from the measured PCG signal. The subsequent section is focused on statistics and comparing analysed data. In the final part, there is a conclusion about the results of the heart sound detection depending on different sensor placement and the used methods.

1 PCG Signal

Physiological events leading to the genesis of PCG signal and PCG signal properties will be discussed in this chapter.

1.1 Cardiac Cycle

In simple terms, the heart can be viewed as a two-pump system. The first pump (the right one) enables pulmonary circulation that means circulation of blood between the heart and the lungs. The second pump enables systemic circulation that is circulation of blood between the heart and the rest of the body.

Cardiac cycle consists of two periods. The first one is systole (pumping) which indicates contraction of chambers. The second period is diastole (filling) which indicates relaxation of them.

1.1.1 Systole period

After previous diastole period **isovolumetric contraction** stage occurs. The left ventricle is filled with the blood from the left atrium. Across ventricular myocardial cells is action potential spread and starts contracting the cardiac muscle cells. Due to contraction the level of the pressure inside both ventricles (left and right) increases rapidly and exceeds the pressure in the atria. The resulting pressure gradient inflicts a short-term change in the direction of blood flow from the ventricles to the atria. This event causes the closure of the atrioventricular valves. The semilunar valves are also closed in this stage because the ventricular pressure is lower than the pressure in large arteria. As all valves are closed, blood in the ventricles cannot be ejected out which causes that the volume of blood remains the same in the heart (isovolumetric contraction). On the other hand, the pressure in the ventricles increases rapidly leading to the start of the next stage.

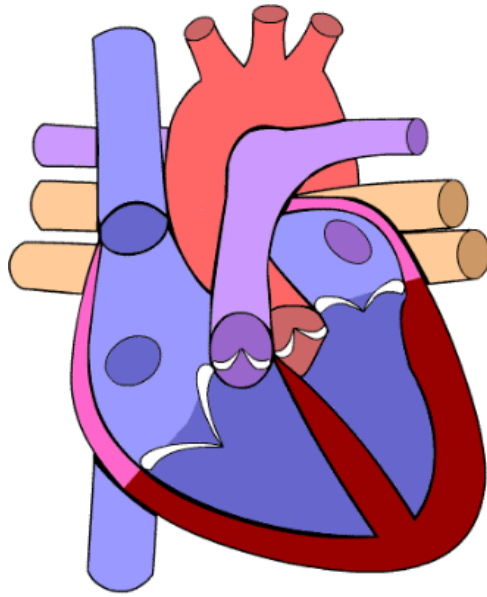


Figure 1: Isovolumetric Contraction

The stage of **ventricular ejection** occurs when the pressure in the left ventricle exceeds the aortic pressure and the pressure in the right ventricle exceeds the pressure in the pulmonary artery. It inflicts the opening of the semilunar valves (the aortic valve and the pulmonary valve). After that, blood is rapidly ejected from the left ventricle to the aorta and from the right ventricle to the pulmonary artery. The contraction from the previous stage is still persistent and, thanks to that, after opening the semilunar valves the pressure in the ventricles remains high, even if the volume of the blood in the ventricles is rapidly decreasing. The level of pressure in the ventricles is higher than pressure in atriums and, therefore, the atrioventricular valves remain closed.

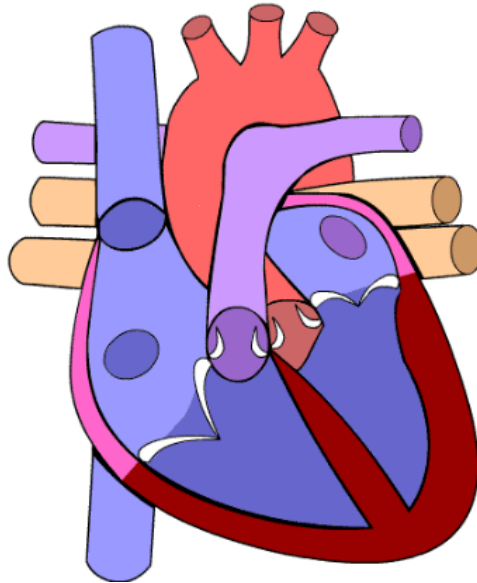


Figure 2: Ventricular Ejection

1.1.2 Diastole period

The level of pressure has been decreasing since the previous stages. Inertia of blood causes for the short time the flowing of blood even after the pressure in arteria exceeds the pressure in the ventricles. After this short time the aortic and pulmonary valves are closed, the systole period ends and the diastole one begins with **isovolumetric relaxation**. The atrioventricular valves are closed too so every valve is closed. Although the pressure in the ventricles is decreasing rapidly, the volume in the ventricles remains the same.

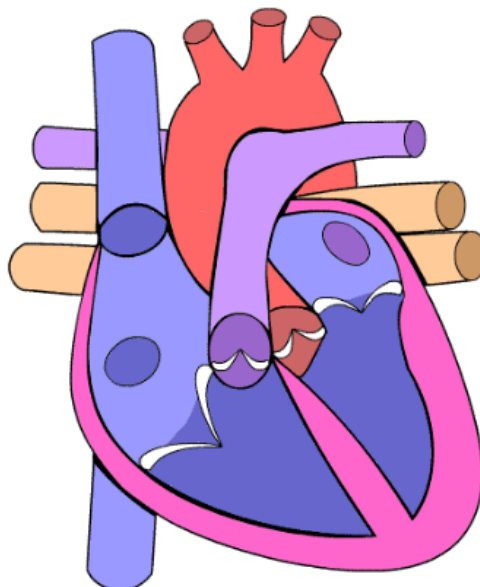


Figure 3: Isovolumetric Relaxation

Rapid ventricular filling occurs when continuously decreasing pressure in the ventricles falls under the level of the pressure in the atria. It causes the atrioventricular valves opening (the semilunar ones are still closed). The ventricles are rapidly filled with blood which was previously stored in the atria. Even if the volume changes rapidly the pressure inside the ventricles remains same (the diastolic pressure) because the cardiac muscle cells are relaxed.

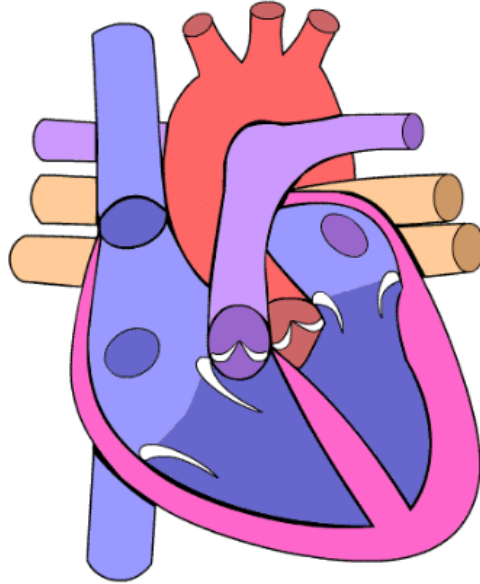


Figure 4: Rapid Ventricular Filling

After that, all the stored blood from the atria flows to the ventricles, the **passive ventricular filling** stage begins. As in the previous stage, the atrioventricular valves remain open and the semilunar ones are closed.

The last stage of the diastole period is the **atrial contraction**. The passive filling stage ends and the active filling starts due to the contraction of the atrial myocardium cells contraction. The volume of blood in the ventricles is increasing but the pressure remains the same (the ventricular myocardium cells are relaxed).

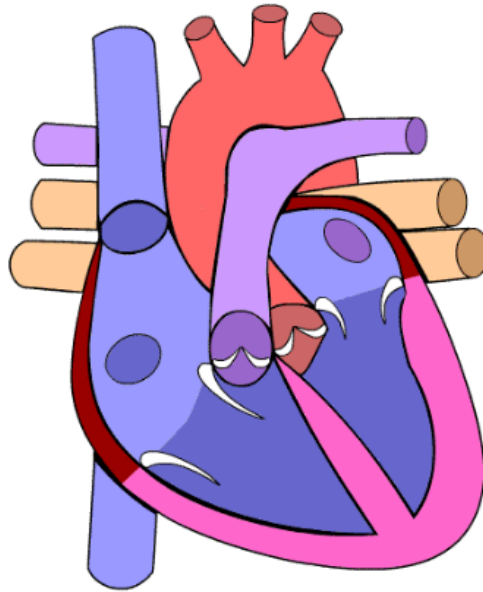


Figure 5: Atrial Contraction

The last three stages are often collectively referred to as the **filling stage**. There is many ways how to look at the processes in the heart. The pressure changes can be measured in the ventricles and the atria but also in arteries and veins. Electrical potential of the heart can be viewed on ECG and heart sounds can be measured using the phonocardiograph. The last two options will be discussed further on.

[1, 4, 12]

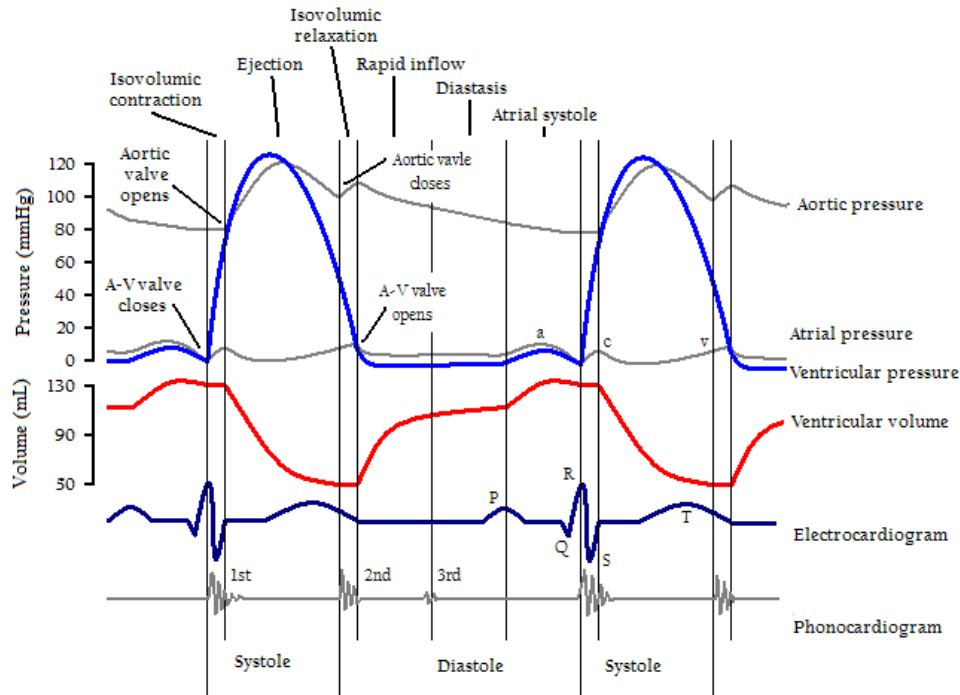


Figure 6: Cardiac Cycle

1.2 Heart Sounds

Characteristic heart sounds are produced during the heart activity (systole and diastole). They are produced because of the opening and closing heart valves, flowing blood in the heart (more precisely by changes in blood flow or flow characteristics) and also by vibrations of the heart muscles. Physical principle of the origin of heart sounds is bumping and moving of the blood volume where there is vibration that wakes up standing waves that we perceive as sounds (short termed, approximately 0.1 second) and murmurs (long termed, longer than 0,1 second). During the heart activity there are four types of sounds. The first two sounds (the primary heart sounds) are easily hearable using the stethoscope. The last two sounds (the extra sounds, gallop sounds) are not always present and it is necessary to have a phonocardiograph to analyse them

1.2.1 First Sound

The first sound has the longest duration of all sounds. The duration is between 0,1 - 0,17 seconds and the frequency range is 25 - 45 Hz (sources also indicate 24 - 104 Hz). The first sound starts at the beginning of the ventricular systole (systolic sound) and it occurs shortly after R peak on an electrocardiogram (that is about 40 - 70 ms after the beginning of the QRS complex).

The first sound is caused by the closing atrioventricular valves probably by the vibrations set up in the valve cusps, chordate, papillary, muscles, and ventricular walls before aortic ejection. The closing of the atrioventricular valves (mitral and tricuspid) is asynchronous and as a result of it there is a split (time delay) between the two components of S1 sound. The delay is 20 - 30

milliseconds and it is very important for diagnostic purposes. The split is usually a normal finding and can be heard by approximately 40 - 70 % of the population.

The first sound includes three main phases. Firstly, there is low amplitude sound caused by vibrations of blood volume during closing the atrioventricular valves at the beginning of the isovolumetric contraction. In the second phase, the amplitude is bigger and is associated with the increasing intraventricular pressure during the isovolumetric stage. At the end, there is also lower amplitude which accompanies the beginning of the ejection stage.

The first heart sound is deeper than the rest of the sounds and it is best audible at the apex of the heart and in the fourth intercostal space along the left sternal border.

1.2.2 Second Sound

The duration of the second sound is in the range 0,1 - 0,14 seconds and frequency spectrum is 24 - 104 Hz for a healthy patient. On PCG it occurs at the same time as the end of T wave on ECG.

The second heart sound consists of two high frequency components. The first component results from the closure of the aortic valve and the second one results from the closure of the pulmonary valve at the end of the ejection stage along with the sudden deceleration and vibrations of the blood flow. Time delay between these two components is dependent on patient's breathing cycle. At the top of the inspiratory phase delay can be up to 30 ms long. On the other hand, at the expiratory phase there are components almost side by side in time domain. This phenomenon is caused by reduction of pressure in lungs which is associated with an increase of venous return to the right atrium. Increasing of the venous return leads to better filling of the right ventricle causing longer ejection phase and delayed closing of the pulmonary valve. This phenomenon is well visible on children, as for adults, the components are often merged into one.

The second heart sound is clearly audible in the second or the third intercostal space along the left sternal border.

1.2.3 Third Sound

The third heart sound occurs at the end of rapid ventricle filling. It has low frequency and very low amplitude which means that it is barely audible. It starts approximately 0,1 - 0,12 seconds after the end of T wave on ECG.

The third heart sound comes from the ventricular wall vibration which is vibrating because of rapid blood flow caused by the great pressure difference between the atria and the ventricles.

Under physiological conditions it is audible only for children and young people. For elderly patients this is a pathological condition.

1.2.4 Fourth Sound

The fourth sound (presystolic) occurs at the late diastolic phase just ahead of the start of the first sound. Time location is the same as the end of P wave on ECG.

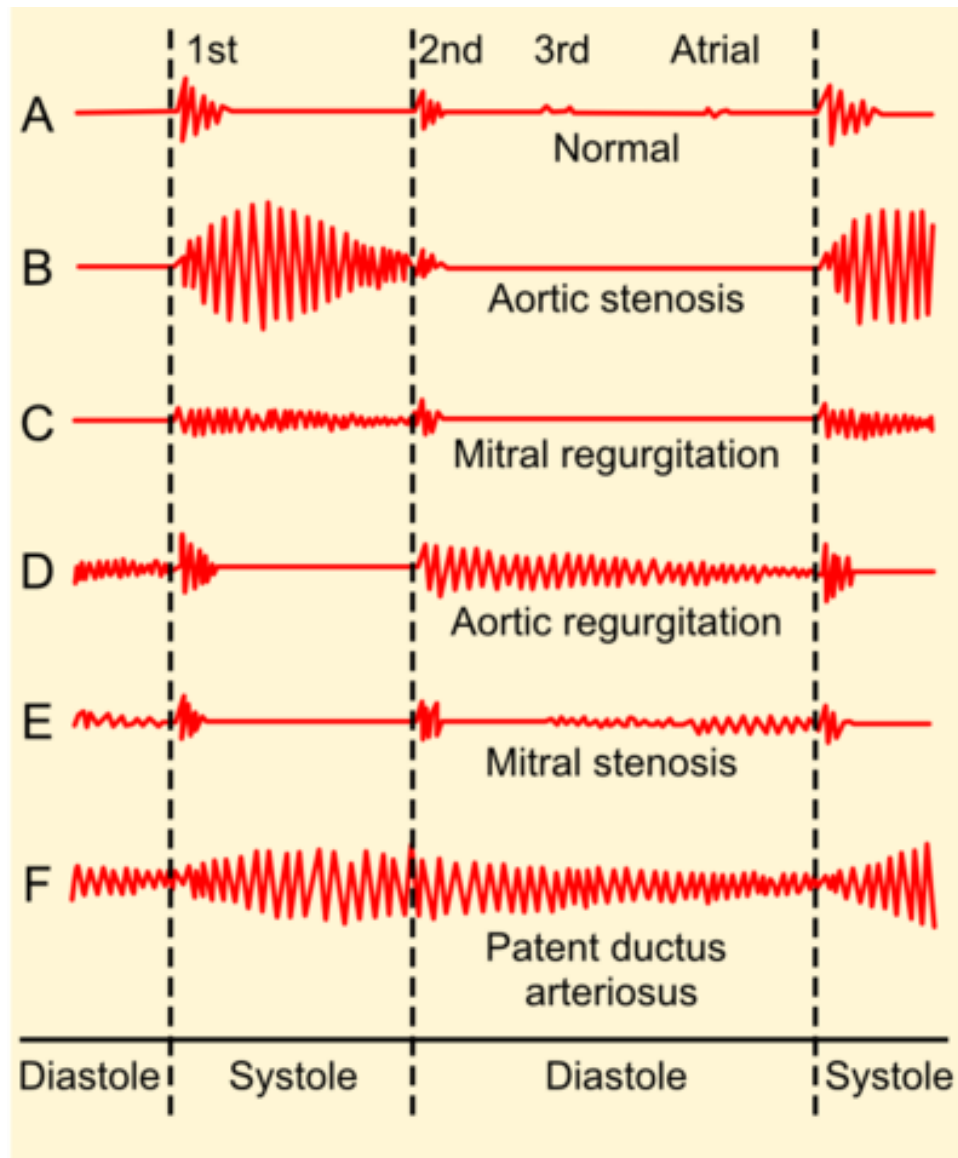
The fourth sound comes from the vibrations of myocardium which is expanded at the atrial contraction. This sound is not audible for a healthy patient, the occurrence of fourth sound indicates a pathological condition.

[1, 2, 4, 6, 12, 13, 14, 46]

1.3 Heart Murmurs

In some physiological but, above all, in pathological conditions there is a change in the nature of the flow causing the vibrations (changes of laminar flow to the turbulent one) which are audible and captured as murmurs. Laminar flow is the flow of viscous liquid in which the liquid particles move side by side as in the layers. During turbulent flow, fluid particles are doing the movement of itself, in addition to the sliding movement, also leads to swirls. The turbulence occurs when the amount and speed of blood flow increases or when the blood vessel diameter is abruptly enlarged or narrowed. The most frequent cause of the turbulence is the change in blood viscosity. Frequencies of murmurs are above 600 Hz.

The character of murmur is mainly given by its spectrum. High-frequency, therefore, high-toned murmurs are created where blood flow is accelerated. On the other hand, low-frequency murmurs, that is, low-toned murmurs, arise at the point where blood flow slows down. We can also classify murmurs by time, localization, propagation of murmur, intensity, quality and dynamic changes.



Phonocardiograms from normal and abnormal heart sounds

Figure 7: Murmurs Overview

The most common murmurs and their causes are shown in figure 9. These include aortic stenosis, aortic regurgitation, mitral stenosis, mitral regurgitation and persistent ductus arteriosus. Aortic stenosis is the thickening of the aortic valve. This defect is characterized by the weakening of the second sound and for systolic murmur spindle shape is typical. Like aortic stenosis also mitral stenosis is caused by the thickening of the valve. Another cause of heart murmur can be aortic and mitral regurgitation. The regurgitation of the valves is characterized by the inability of the valve leaflets to appropriately close themselves (sufficiently tightly) at the

end of systole causing the flow of blood back to the heart.

Heart sounds and murmurs have very low level and frequencies in the range of 20 – 2000 Hz. Disorders in the mechanical functioning of the heart will be reflected in the changes of heart sounds and murmurs. The simplest technique for evaluating heart sound is the auscultation technique (listening evaluation) that does not require any electronic device and it is enough to use a simple stethoscope.

[1, 2, 4, 6, 12, 13, 14, 45]

1.4 Auscultation

Auscultation of the heart is referred to as one of the most important and useful clinical methods of the heart examination. The examination usually takes place in three positions: the patient is lying on the back, lying on the left side with his left hand under his head and sitting.

The heart is usually auscultated in four places that correspond to the auscultation projection of the heart valves but the listening is not limited to these places.

- Aortic region (between the 2nd and 3rd intercostal spaces at the right sternal border) (RUSB – right upper sternal border).
- Pulmonic region (between the 2nd and 3rd intercostal spaces at the left sternal border) (LUSB – left upper sternal border).
- Tricuspid region (between the 3rd, 4th, 5th, and 6th intercostal spaces at the left sternal border) (LLSB – left lower sternal border).
- Mitral region (near the apex of the heart between the 5th and 6th intercostal spaces in the mid-clavicular line) (apex of the heart).

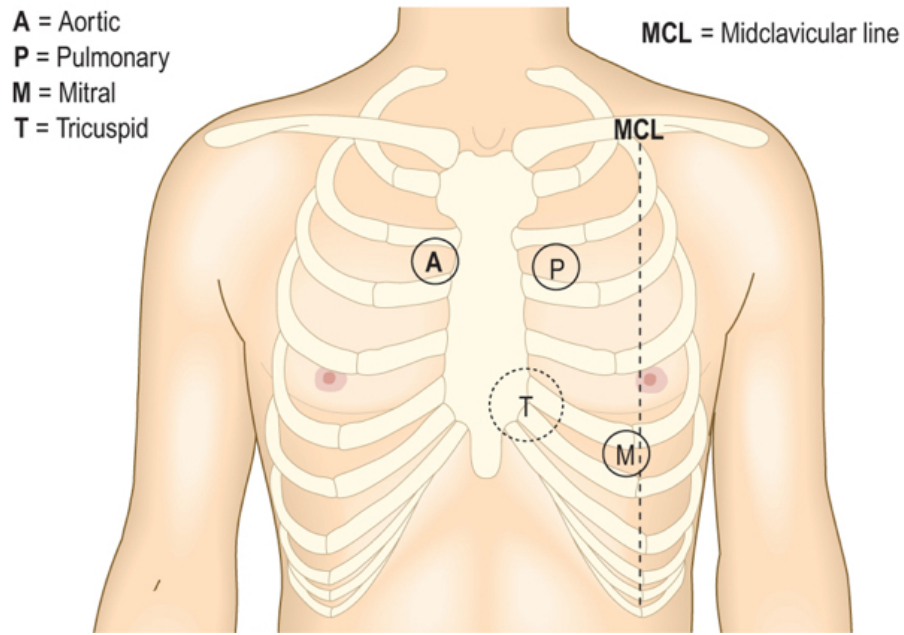


Figure 8: Auscultation Areas

[6, 7, 10, 12, 45]

1.5 Electrocardiography

Electrocardiography is a diagnostic method allowing measuring and recording electrical activity of the heart. It is one of the basal diagnostics methods in cardiology. A graphical representation of heart activity is electrocardiogram. ECG signal is a bio signal of the heart. To understand the genesis of ECG it is necessary to explain the functional electrical conduction system of the heart.

1.5.1 Electrical Conduction System

Rhythmic activity of the heart provides the electrical conduction system of the heart with gradual electrical activation of the cardiac compartments. The electrical conduction system of the heart forms cells called myocytes and also provides for the generation and the spread of action potential. Unlike skeletal muscle the cardiac action potential is not initiated by nervous activity. Instead, it arises in the heart itself from myocytes. Thanks to this automation, we are not able to control the muscles of the heart.

Heart rhythm is produced by action potentials from the sinoatrial (SA) node which is located in the wall of the right atrium. SA node is known as the natural pacemaker and the rate of action potential production estimate heart rate. The frequency of the action potential determines the frequency of heart strokes in a healthy heart. The shape of the sinoatrial node reminds of a drop,

the wider part of which lies at the mouth of the vena cava inferior, the tapered part reaches about half of the atrium.

From the SA node, the electric impulse spreads to the atrium on the atrial myocardium (contraction occurs) and then goes to the atrioventricular (AV) node. The AV node is the only place (in healthy individuals) where electrical energy is transferred from the atria to the ventricles. The AV node is referred to as the secondary pacemaker and indicates the rhythm in the absence of the rhythm from the SA node. The propagation of action potential in the AV node is delayed, this delay is necessary for atrial contraction to be completed and thus to increase the volume of the ventricles before their own contractions. The AV node lies subendocardial in the lower part of the right atrium. Action potential from the AV node spreads through the heart muscle towards the chambers where the Hiss bundle is located in the interventricular septum. The impulses penetrate through the membrane septum between the chambers and the halls and go to Tawara branches (bundle branches). The left bundle is divided into the left anterior fascicles and the left posterior fascicles, the right is not split along the right edge of the interventricular septum. The shoulder ends in Purkinje fibers forming a subendocardial stored net at the level of both ventricles.

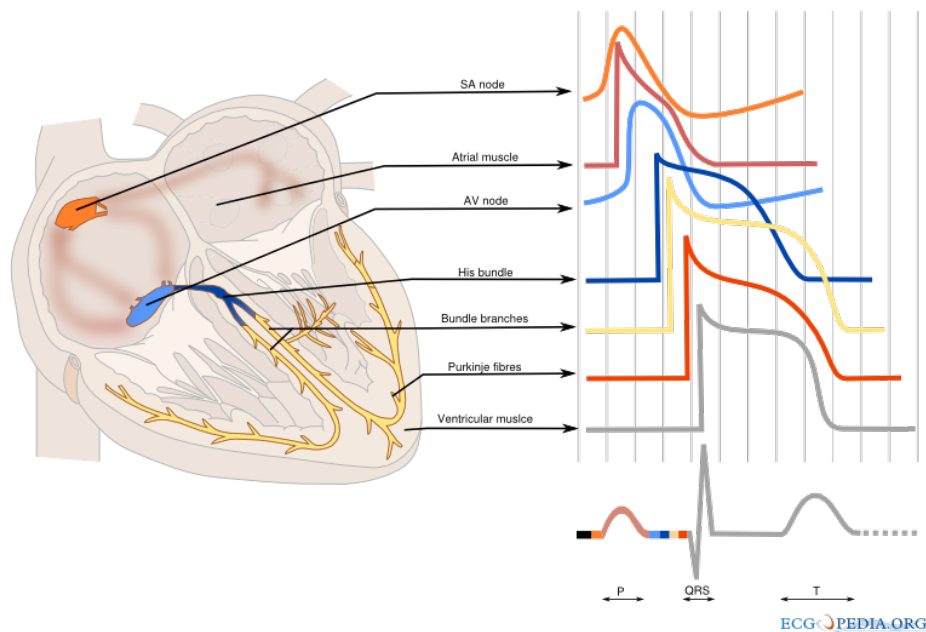


Figure 9: Electrical Conduction System

1.5.2 Genesis of ECG Signal

By spreading the action potential through the electrical conduction system and the surrounding musculature the electric field of the heart develops. Thus, the heart can be imagined as a

generator of this electric field. By measuring the potential of the electric field of the heart and by using of the electrodes we obtain an electrocardiogram.

In a simplified way, the heart can be seen as an elemental electrical dipole then the voltage on the electrodes arranged as the vertices of the Einthoven triangle will be given by a projection of the vector representing this dipole into the individual sides of the Einthoven triangle.

As mentioned above, the action potential arises in a healthy individual in the SA node and spreads as a depolarizing wave across the walls of both atriums and the onset of P wave is manifested on ECG.

At the start of atrial contraction the depolarization of both atria is completed and the end of the P wave can be recorded on ECG. The atriums are then completely depolarized and the electrical excitement is transferred to the AV node. Therefore, in ECG there is an isoelectric line - the PR segment. In the AV node there is a delay in the propagation of the action potential that is necessary to fill the chambers. Prior to the initiation of isovolumetric contraction, the action potential of the AV node passes through the His bundle and Purkinje fibers to the ventricular muscles. The gradual spreading of depolarization to the intraventricular septum and then to the walls of both ventricles is shown on ECG as the QRS complex (ventricular complex). The right ventricle is depolarized first, the depolarization of the left ventricle is slower. At the same time, the repolarization spreads to the heart but it cannot be identified on ECG because it is overlapped by the QRS complex. When the depolarization of the ventricles is complete the atria are fully repolarized. In the ventricular cells, the plateau phase occurs in which the membrane voltage changes very slowly which is shown on electrocardiogram as a flat segment ST. During the slow ejection, the ventricular muscles begins to repolarize, the gradual repolarization occurs asymmetrically between the ventricles (as well as depolarization) and manifests itself as a T wave. Electrocardiogram can distinguish lines (isoelectric line), waves (P, T, U), peaks (Q, R, S), intervals and segments.

[1, 2, 3, 6]

1.6 Phonocardiography

Phonocardiography is a diagnostic graphical method of recording sounds and echoes that accompany mechanical vibrations originating in the heart and vessels. It is used to register heart sounds and murmurs for diagnosis of heart diseases. Since both heart sound and murmurs have frequencies ranging from 20 to 2,000 Hz they cannot all be captured using a conventional stethoscope (stethoscope). A phonocardiograph is therefore used for recording.

1.6.1 Phonocardiograph

Phonocardiograph is a device that measures and records sound signals using a non-invasive method consisting of a microphone in the surface of the chest wall. The microphone is attached to the usual auscultatory points of the heart after previous auscultation with a stethoscope.

The main advantage of phonocardiography is to record sound signals that are below our hearing threshold. Another undoubted advantage is more accurate analysis of the audio signals, especially their timing in the heart cycle, as well as the possibility to store this information for documentation.

The conventional phonocardiograph consists of three parts – a microphone, an amplifier and filters. A phonocardiograph can work independently (electronic stethoscopes) or can be a part of an ECG device.

The microphone transforms acoustic (mechanical) oscillation (acoustic pressure) into an electrical signal. This is further filtered. The most commonly used microphone is crystal (piezoelectric) and dynamic (moving-coil microphone).

A crystal microphone uses a piezoelectric effect. Its most important part is crystals of Rochelle salt (potassium sodium tartrate tetrahydrate) which are coated on both sides with conductive plates (electrodes). Due to the deformation of the crystal the voltage occurs on these electrodes. The piezoelectric effect also works in the opposite way, if the voltage is applied to the electrodes, the crystal is stretched or shrunk depending on the polarity. By gluing such two plates one shrinks when the other one stretches and a piezoelectric pair is formed. Plates are often shaped into disks, these are electrically connected in parallel (the charges are added together) and mechanically in series. The dependance between the change of acoustic pressure and the piezoelectric charge is linear. If the membrane is added to this pair a crystal microphone is made. Acoustic (pressure) wave impact generates an alternating voltage in millivolt units which is proportional to the amplitude of the pressure wave. The frequency range is approximately 0 to 10 kHz. Internal microphone resistance of this type is high (in the order of megaohms) so the input resistance of the amplifier must be high. The microphone is connected to the amplifier with a shielded cable that reduces electromagnetic radiation (and thus electrical noise). Since we do not use the entire frequency range (especially higher frequencies), cable length and capacity are not critical. The disadvantage of the crystal microphone is higher sensitivity to heat and humidity.

A dynamic microphone uses another principle of the acoustic wave transformation to the electrical ones. The dynamic microphone diaphragm is coupled to a cylindrical coil that moves in the permanent magnet gap. In such a movement electrical voltage is induced in the coil. Unlike the crystal microphone the dynamic microphone has low internal resistance (in the order of ohms) and its conduction (due to low impedance) is almost insensitive to interfering voltage. The microphone is connected to the amplifier input via the transformer to obtain higher output voltage.

The output of phonocardiography is phonocardiogram.

1.6.2 Phonocardiogram

Phonocardiogram is a graphical record of heart sound, murmurs and other sounds caused by activity of the heart, blood flow and other factors (respiration).

The sounds and murmurs occurring during heart activity can be seen as an amplitude-modulated signal. In this signal, the signal envelope is interesting from the diagnostic point of view, the acoustic vibrations themselves are only carriers of frequencies. Heart sounds are in lower frequency range than murmurs which, on the contrary, fall into the higher frequency spectrum.

[2, 4, 8, 12, 47]

1.7 Used Equipment

For the PCG and ECG recording, the data acquisition system from AD Instruments was used for the purposes of the thesis.

1.7.1 Hardware

The heart of the acquisition system was PowerLab 16/35. It allows to connect the analog output from the microphone or ECG electrodes, digitize them and thus enable them to be measured and processed in a PC (or other platform). An overview of its selected parameters is in the following table:

Table 1: Technical Parameters of PowerLab 16/35

Data communication:	USB 2.0
Analog input channels:	16
Single ended inputs:	16
Differential inputs:	4
Input voltage range:	± 2 mV to ± 10 V
ADC resolution:	16 bit
Max. sampling rate:	200 kS/s
Frequency response:	-3 dB (25 kHz, 10 V)
Output voltage:	± 200 mV to ± 10 V

A cardiomicrophone MLT201 was used to measure the PCG signal. An overview of its selected technical parameters in the table below.

Table 2: Technical Parameters of Microphone MLT201

Maximum excitation:	± 10 V
Conversion factor at 100 Hz:	100V/s
Operating frequency:	10 to 600 Hz
Dynamic range:	0.01 to 10 m/s
Variation in frequency response:	± 3 %
Resonant frequency:	3.4 kHz
Amplitude nonlinearity at 10 Hz:	± 3 %
Operating temperature:	15°C to 45°C
Connector:	8-pin DIN

1.8 Software

LabChart software is also a part of the PowerLab system. It allows to see and analyse a record of all devices connected to the PowerLab Acquisition System at the same time. Thanks to the easy-to-use and real-time measurement and other features it is well applicable for measurement and the results can be exported to many formats.

The Matlab software was used to analyse the signal exported from LabChart. [36]

2 Data Acquisition

An important part of this work was the acquisition of data. Compared to many other studies, the four to twelve PCG signals (from different positions on the chest) was measured with ECG at the same time. To get as many heart cycles as possible for the analysis, the duration of each measurement was at least 2 minutes which also surpassed time in many other studies. For data acquisition, two auscultation sites were made.

2.1 Auscultation Site A

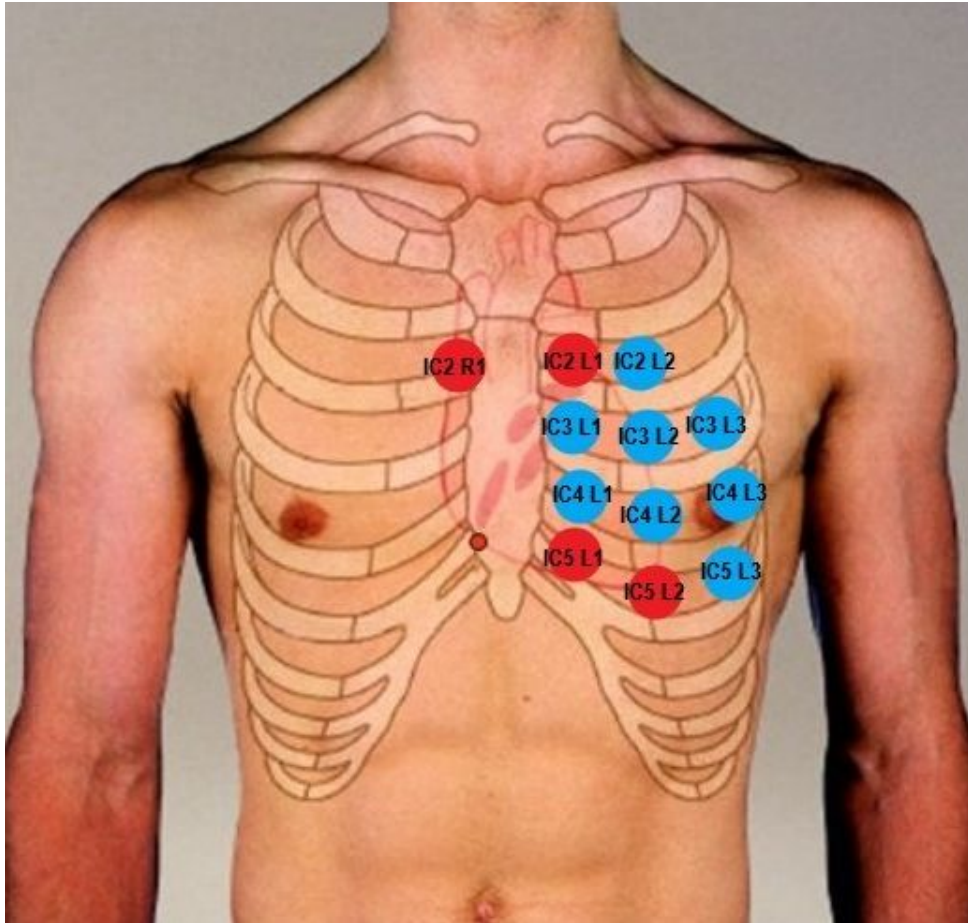


Figure 10: Auscultation Site A

The auscultation site is demonstrated on figure 10 above. All 12 available sensors were used as measuring tools in this auscultation site. The location of the sensors was chosen to include 4 standard auscultation areas (red points) and to well map the heart area. Also, the points were chosen so that they were easily identifiable and descriptive and allowed to repeat the same sensor placement for other measurements and patients. As reference there are considered intercostal areas and distance from the sternum. The form of the area designation is described in the table

bellow. Similar sensor deployment was also used in the previous energy measurement study. [48]

Table 3: Explanatory Notes to the Auscultation Site

Abbreviation in the Description	Meaning	Values
IC	Intercostal space	-
2,3,4,5	Number of IC	2nd intercostal space, 3th intercostal space...
R,L	Parasternal area	Right or left
1,2,3	Distance from sternal bone	1 = lateral sternal line 2 = mid clavicular line 3 = axially reversed line to lateral sternal axis (by mid clavicular line)

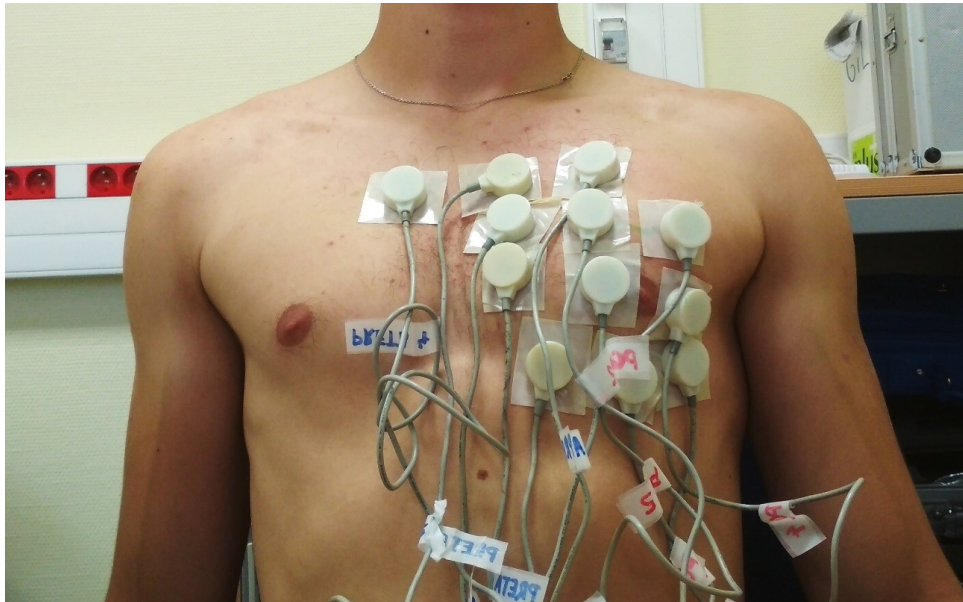


Figure 11: Measuring Using Auscultation Site A

2.2 Auscultation Site B

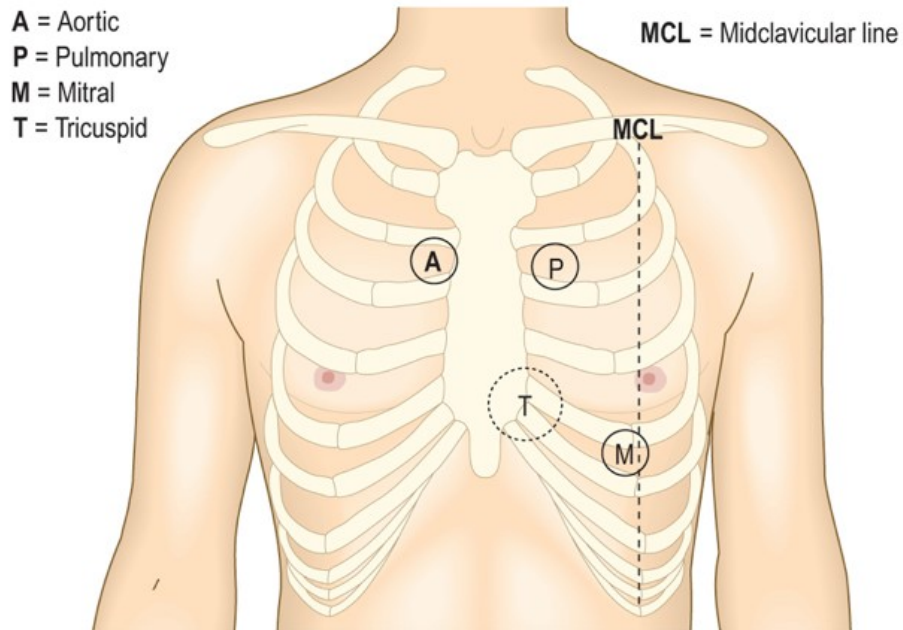


Figure 12: Auscultation Site B

Auscultation site B includes 4 reference (standardized) heart sound measurement areas. This site was mainly used for the time-consuming measurement of degraded data, with the help of this network a greater comfort of patients was achieved. This is the ergonomic version of the previous auscultation site. This site has a benefit that it makes the data analysis simpler and data acquisition easier.

2.3 ECG Measuring

Since the detection algorithm uses synchronization with the R peak and the T wave it was necessary to measure ECG in addition to PCG. Measuring of ECG was performed using the Eindhoven's limb lead I (on Figure below). In the lead I, the left arm electrode is the positive pole and the right arm electrode is the negative pole.

Disposable electrodes (Ag/AgCl) were used for ECG measuring.

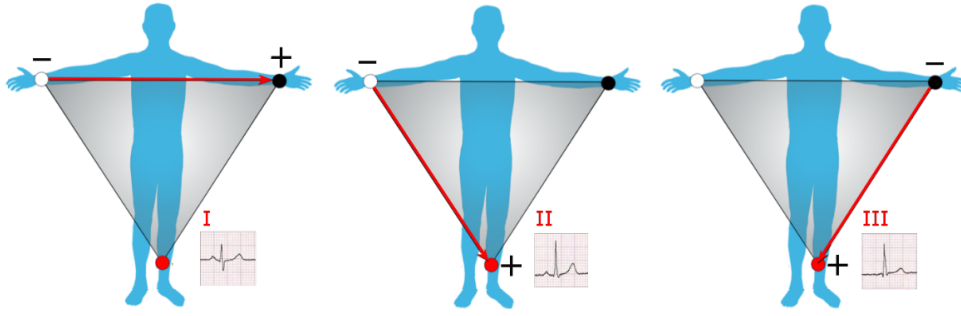


Figure 13: ECG - Limb Leads

2.4 Measurement Protocol

Each measurement was performed in a quiet laboratory (without a special acoustic shielding). Before the arrival of a patient, the acquisition system with an appropriate number of sensors was set up. Then the patient came and the appropriate auscultation places were found using palpation and marked. The entire measurement was performed at the sitting position of the patient. Each measurement took at least 2 minutes and then the results were saved. The patient could relax and stretch his body. After that, the sensor mounting was checked and re-attached if necessary. If the patient agreed other measurements were taken to obtain as much data as possible for further analysis.

2.4.1 Sensors Attachment

The problem with attachment of the sensors was very important. Different types of attachments were tested providing different results.

Firstly, the sensors were attached with an adhesive tape over them. Different types of tapes were tested. The tapes of a rustling material were evaluated as unsuitable because they produced disturbing sounds when the chest wall moves so that the tape sounds were on the record of PCG hardly recognizable from the heart sounds. Also, the tapes which were low-sticky and which, during the measurements, came unstuck were proved to be inappropriate. The use of the kinesio tapes that are elastic and resistant to the movements of the chest wall has proved effective. Repeated tests, however, showed that using a tape over the sensor cannot achieve the standardization at the level of force applied by the sensor to the chest wall. These pressure differences proved to be very important because they affected the quality of the output signal (the noise level and the magnitude of the measured amplitude) much more than, for example, minor differences in the location of the sensor. Despite the importance of the issue many studies do not specify the method of attaching PCG sensors to the patient.

For further measurements in this work, a thin pad made of a double-sided adhesive tape was used as the attachment. This pad was placed between the patient's chest and the PCG sensor.

This method guarantees the standardization of the attachment since the sensor pushes on the chest wall always with the same force.

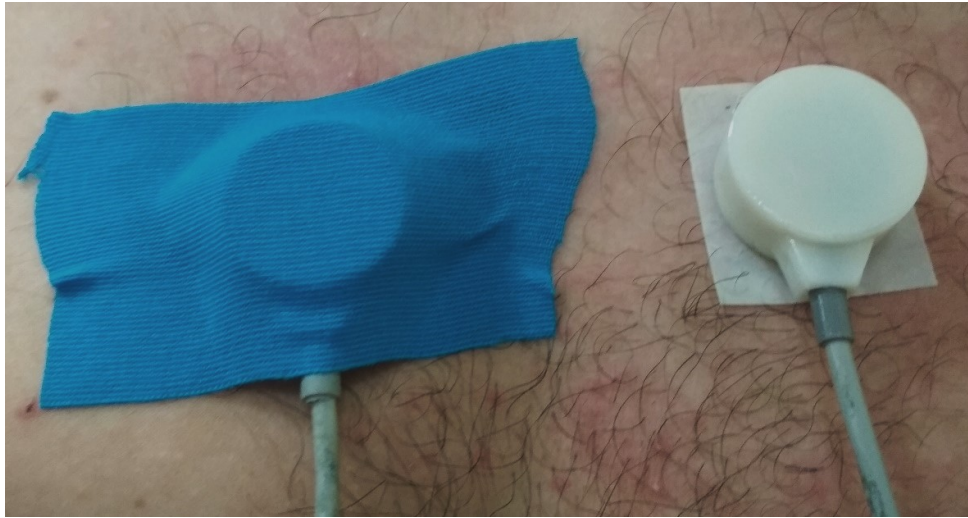


Figure 14: Different Types of Attachment

2.5 Measuring of Damaged data

A part of this work was not only measuring data in ideal conditions but also simulating conditions that can lead to the signal degradation. For this reason, it was necessary to propose a measurement protocol that would define various possible situations leading to the influence of the measured signal. Table 4 containing the different test situations is bellow.

Table 4: Measuring Protocol for Damaged Data

Situation	Total length (min)	Start (min)	End (min)
ECG unattachment - neutral electrode	4	2:00	3:00
ECG unattachment - active electrode	4	2:00	3:00
PCG unattachment	4	2:00	3:00
Noisy room (one source 60 dB, 1 meter)	4	2:00	3:00
Coughing (2 seconds, repeat every 15 seconds)	4	2:00	3:00
Ringling of the phone (one source 70 dB, 1 meter)	4	2:00	3:00
Breathing apnea (15 seconds, 2 repetition)	4	2:00	3:00
Breathing tachypnoea (10 seconds, 2 repetition)	4	2:00	3:00

As the table suggests, the degrading situation / event itself was preceded by a 2-minute measurement under the ideal conditions, and after the degrading situation / event, the measurement continued for 1 minute under the normal conditions. This measuring procedure was

performed because of the development of the rupture finding algorithm in the next research (not part of this work). As well as in the measuring of the normal (undamaged) data, a patient was in the sitting position and the way of the attachment of the sensors remains the same (the double-sided adhesive tape). Each measurement was done twice. Thus, for each patient, 64 minutes of the pure signal time (5 channels - 4 PCG and 1 ECG) with 8 possible degrading situations were measured with this protocol. For the measurement purposes, the auscultation network B was chosen because of the time reasons, the patient's comfort and later analysis of the data. However, the aim of this work was not to analyse such degraded signals but only to measure them.

3 Heart Sound Detection

To compare and analyse the difference between the location of the PCG sensors, the first two heart sounds were chosen as the test parameters, respectively, their time location and amplitudes. These sounds were chosen because they occur in all healthy individuals and are relatively easy to detect.

3.1 Existing Methods for Detecting Heart Sounds

Many scientific articles deal with the detection of the first two heart sounds, or other elements of phonocardiogram, such as murmurs and another pathological phenomena. There is a large amount of methods for detecting S1 and S2.

These methods can be divided according to whether they use a different signal than PCG (ECG, carotid / jugular pulse etc.) - multiple source or whether they use only PCG (one channel, multiple channels) for the detection - sole source.

In the heart sound detection, there are several basic approaches to get information about heart sounds. One approach includes methods which use the signal envelope for analysing heart sounds. Even though the signal envelope does not contain all the information of the original signal it has a great diagnostic importance because it emphasizes the basic heart sounds. There are many ways how to obtain the envelope of PCG. Commonly used methods are based on the homomorphic filtration or the signal energy computation (Square energy, Shannon entropy, Shannon energy). Also, Hilbert transform can be used for the envelope detection.[6, 11, 15, 18, 24, 28, 29, 33, 35, 49]

Detection methods could be also based on the Short Time Fourier transformation and the Wavelet transformation (or more flexible Wavelet packet decomposition). To investigate the exact features of the heart sound these methods use both time - frequency representation of the signal. The signal is usually decomposed into a tree of a few levels using corresponding wavelets (in case of the Wavelet transform) and then the wavelets which has good time locality and high energy concentration are chosen to reconstruct the signal. After this process (it can be a part of preprocessing) the output is further processed and analysed by many possible different ways.[12, 17, 23, 25, 26]

More sophisticated methods include the methods based on probabilistic models such as Hidden Markov Models (eventually duration-dependent hidden Markov model) as a probabilistic finite state-machine. The Hidden Markov models (HMM) is used in this group of methods for the segmentation of heart sounds. The basic idea is that the HMM assumes a double stochastic process consisting of an underlying hidden Markov process which generates an observable stochastic output. This model corresponds well to the current task where the state of the heart is unknown but the stochastic output, the heart sounds, is observable.[20, 27]

Another approach to detect heart sounds is the usage of neural networks. Neural networks can be used for the classification of the heart sound obtained by some of the methods mentioned

above. The main use is in solo source signals where there is no additional information about heart cycle and the classification without using neural network is very difficult. There are important differences in approaches of methods using neural network for a heart sound analysis as well as differences in variants of neural network itself.[21, 30, 31, 32]

3.2 Heart Sound Detector Realization

When choosing the method of realization of the heart sound detector it was approached with regard to the acquisition options and the sensor output requirements. For the study, it was necessary to detect the first two heart sounds and to classify them correctly. The acquisition system allowed up to 12 PCG within ECG channel to be measured. For the most accurate reliability of the detector the multimodality of this acquisition system was used which means that synchronous ECG and PCG capture enables the use of the ECG signal as a time reference to the PCG signal to improve the detection of the heart sounds.

To analyse the PCG signal the signal envelope detection method was chosen using the Normalized Averaged Shannon Energy, where the classification and more accurate detection ensure the synchronization with the R peak and the T wave on cardiogram. The method of the envelope detection using the Averaged Shannon energy was selected because this method is very popular in PCG processing and there are many studies demonstrating the great effectiveness of this method. [15, 22, 24, 33, 34, 49]

Using this method in combination with the ECG synchronization allows, by a simple set of different parameters, the analysis of very variable PCG signals measured on standardized but also non-standardized locations and measurement of the heart sounds. Also, the proposed method is computationally relatively fast even in the case of 4-minutes length signals.

The entire detector was implemented in the Matlab programming environment. The simplified block diagram below describes the detector function. The individual blocks are described below.

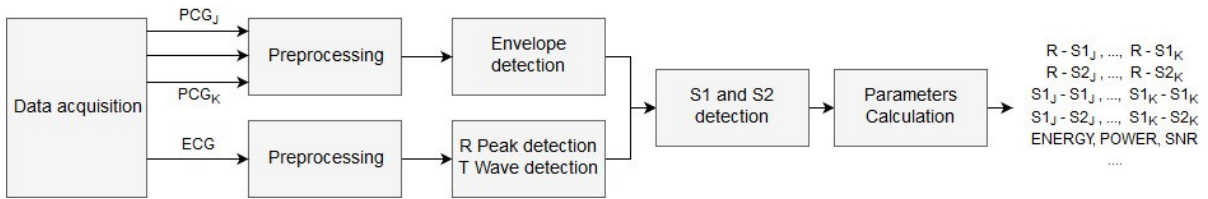


Figure 15: Heart Sound Detector - Block Diagram

3.3 PCG Preprocessing

Prior to extracting the envelope from a phonocardiogram the signal must be pre-processed. The measured signal contains not only the components corresponding to the sounds generated by the activity of the heart but also other interfering components that are undesirable to obtain the envelope. These are disturbing sounds from muscle activity, breathing, movement of the sensors

on the subject (patient), or ambient sounds (speech, music) and more. Some disturbing sounds can be eliminated by adjusting the conditions for the measurement, but not all. Therefore, the PCG signal needs to be pre-processed.



Figure 16: PCG Preprocessing - Block Diagram

3.3.1 Filtering

The first preprocessing step is filtering to suppress undesirable components. A bandpass FIR filter with Hamming Window and filter order $n=128$ was used for the filtration. This filter retains only signal components in the range from 25 to 145 Hz. This range was chosen with respect to preserving the main components of the first and the second heart sound and suppressing the components which are unimportant from the point of view of S1 and S2 detection. Previous studies have proven that the dominant frequencies are ranging from 24 - 104 Hz for S1 and 24 - 144 Hz for S2. It means that most of the signal energy lies below the frequency of 150 Hz. [13].

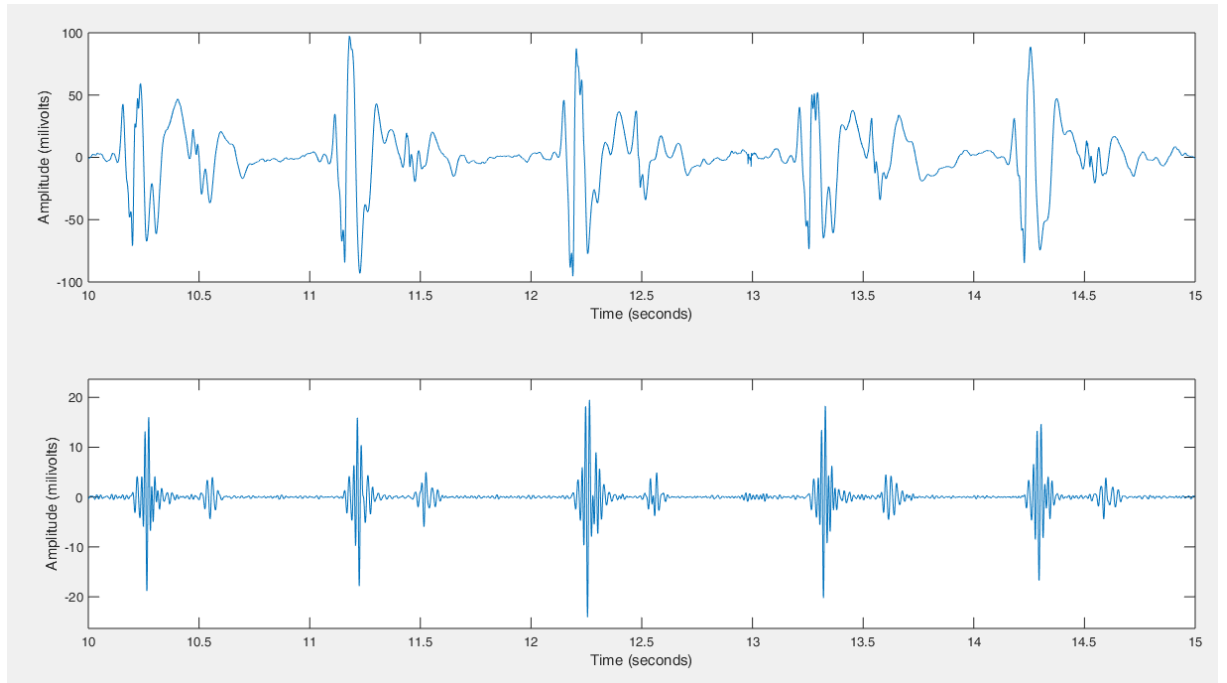


Figure 17: PCG Filtration

3.3.2 Normalization

The next step of the signal preprocessing is signal normalization. Normalization in general means that values are adjusted to common scale. In the case of the PCG signal is the signal normalized to absolute maximum according to the equation 1.

$$pcg_{norm}(k) = \frac{pcg(k)}{\max(|pcg(k)|)} \quad (1)$$

It follows the equation that the PCG amplitude after applying the mathematical relationship above will be in the range from -1 to 1.

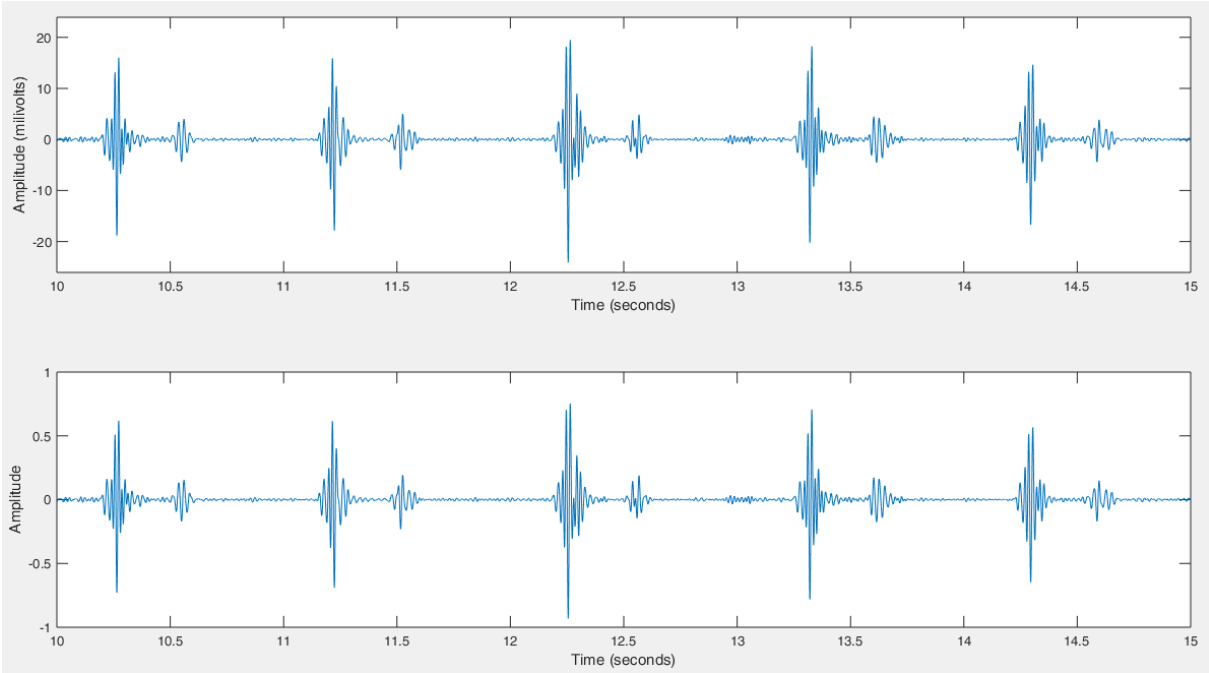


Figure 18: PCG Normalization

3.3.3 Segmentation

Before calculating the energy required to extract the envelope the signal needs to be split into segments. The length of the signal was firstly modified to be divisible by 32. Then the PCG signal was divided into 32-sample segments throughout the normalized signal with 2-sample segment overlapping. That is, at a sampling rate of 1kHz makes a 0,032-second segment throughout the signal with 0,002-second segment overlapping. This overlapping was chosen as a compromise between the acceptable calculation speed and the number of segments obtained that determine the sampling rate of the envelope. The overlapping caused the down sampling the envelope over the original signal from 1 kHz to 500 Hz sample rate. The mechanism of segmentation for the first three segments is described in the figure bellow.

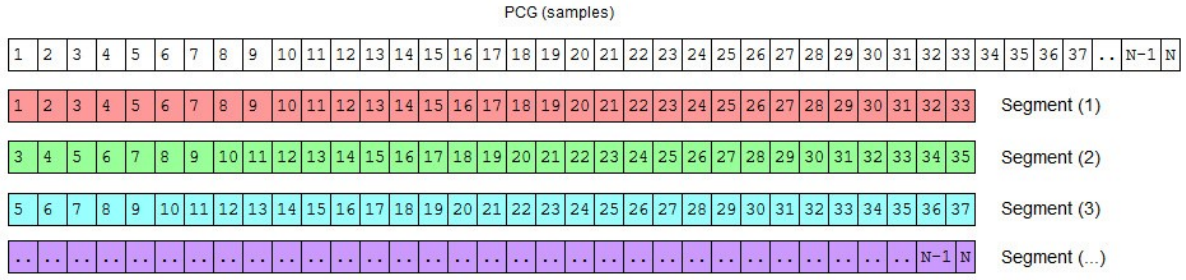


Figure 19: PCG Segmentation

3.3.4 Extraction of the Heart Sound Envelope

The extraction of the heart sound envelope is implemented by calculating the normalized average Shannon energy. There are different methods of calculating the envelope of the normalized signal obtained through the equation 1. In the figure 20, there are shown some of them. Because of the symmetry of the results the negative part is ignored.

The figure below is drawn based on the following definitions, here x is the normalized signal, which has the real value from -1 to 1.

Absolute value: $E = |x|$

Square Energy: $E = x^2$

Shannon Entropy: $E = | -x | \cdot \log |x|$

Shannon Energy: $E = x^2 \cdot \log x^2$

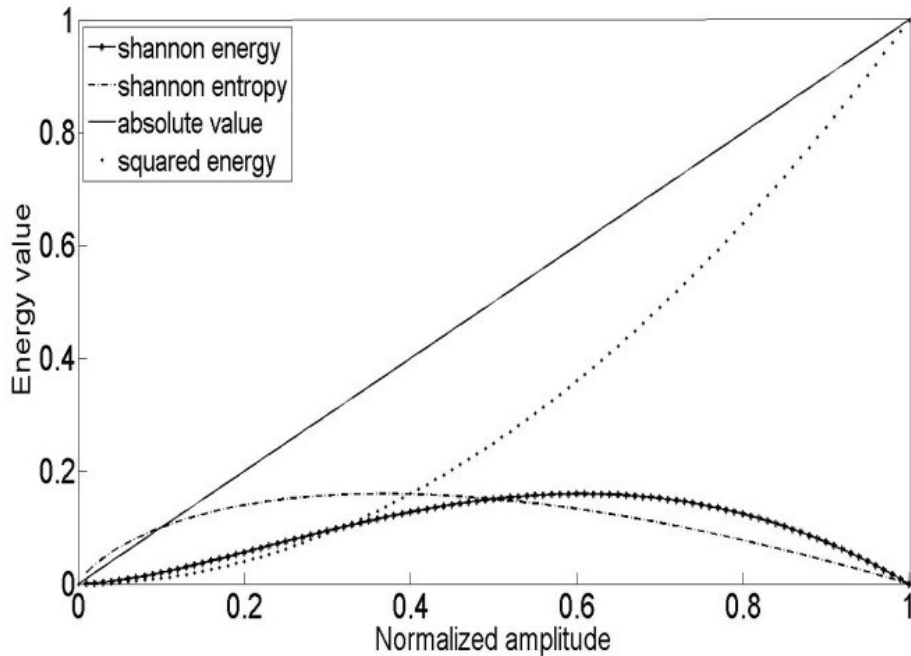


Figure 20: Comparison Between Different Envelope Methods

Figure 20 provides a basic framework for comparing the efficiency of various envelope detection methods. The squared energy method associates the exponential weighing factors to the high intensity components which will pose difficulty in isolating the low intensity components. The absolute value technique associates the same weighing factor to all components making it difficult to separate low from high amplitude signals. The Shannon entropy method attenuates the high intensity signal since it gives more weights to the low intensity signal. However, it is evident from the graph that the Shannon energy method emphasizes the medium range amplitude components and attenuates the low intensity signal more than the high intensity components.

Shannon Energy can absorb the magnitude of oscillations of high intensity as well as those in low amplitudes. The square and the absolute value of the signal samples promotes oscillations of high amplitude more than those of low amplitude. To improve this beneficial effect we can standardize or normalize this energy. [15, 22]

The average Shannon Energy is standardized by the following relationship:

$$E_S = -\frac{1}{N} \cdot \sum_{i=1}^N \cdot x_{norm}^2(i) \cdot \log x_{norm}^2(i) \quad (2)$$

The normalized average Shannon Energy is standardized by the following relationship, where μ is the average value of energy E_S of the signal, σ is the standard deviation of energy E_S of the signal:

$$E_N = -\frac{E_S - \mu}{\sigma} \quad (3)$$

For extraction of the heart sound envelope formula has been improved according to 2.

$$E_S = -\frac{1}{N} \cdot \sum_{i=1}^N \cdot |x_{norm}(i)|^{\frac{5}{2}} \cdot \log |x_{norm}(i)|^{\frac{5}{2}} \quad (4)$$

With the change of order in the equation, the resulting signal envelope changes. Previous studies have shown the average Shannon energy can attenuate the effect of low value noise. And the higher the order of x in formula is, the better the effect of the weakening of murmurs is. In order to weaken the influence of heart murmurs the order of x is increased. Although the higher order of x causes better effect the intensity of S2 should not be high enough. In a simplified way, with the order in the formula, the envelope is smoother and less sensitive to murmurs but the amplitude of the individual lobes decreases. In the figure bellow, the effect of the order for envelope detection is demonstrated. The comparison shows only small differences between formulas with the order number n.

This formula was chosen as a compromise between the common formula for calculating Shannon energy and the formula proposed in the study by Wang. [24].

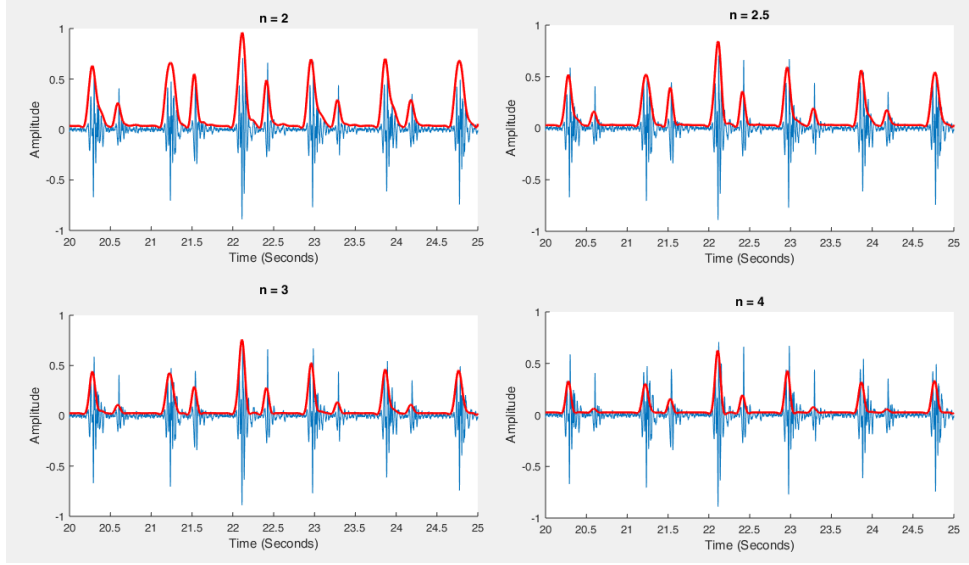


Figure 21: Comparison of Calculated Envelops Using Different Order

After extraction of the heart sound envelope the envelope is filtered. The lowpass FIR filter with Hamming Window and the filter order $n=128$ was used for filtration. Cut off frequency was set to 20 Hz. For the next steps it is necessary to obtain low frequency envelopogram because the peaks in the envelope will be detected as S1 or S2 in the next steps. Without envelope filtration there could be the 2 peaks for 1 heart sound (for example split S2) on envelopogram and that is undesirable for the purpose of this work. In the figure bellow, the comparison between an unfiltered envelope and a filtered envelope is shown.

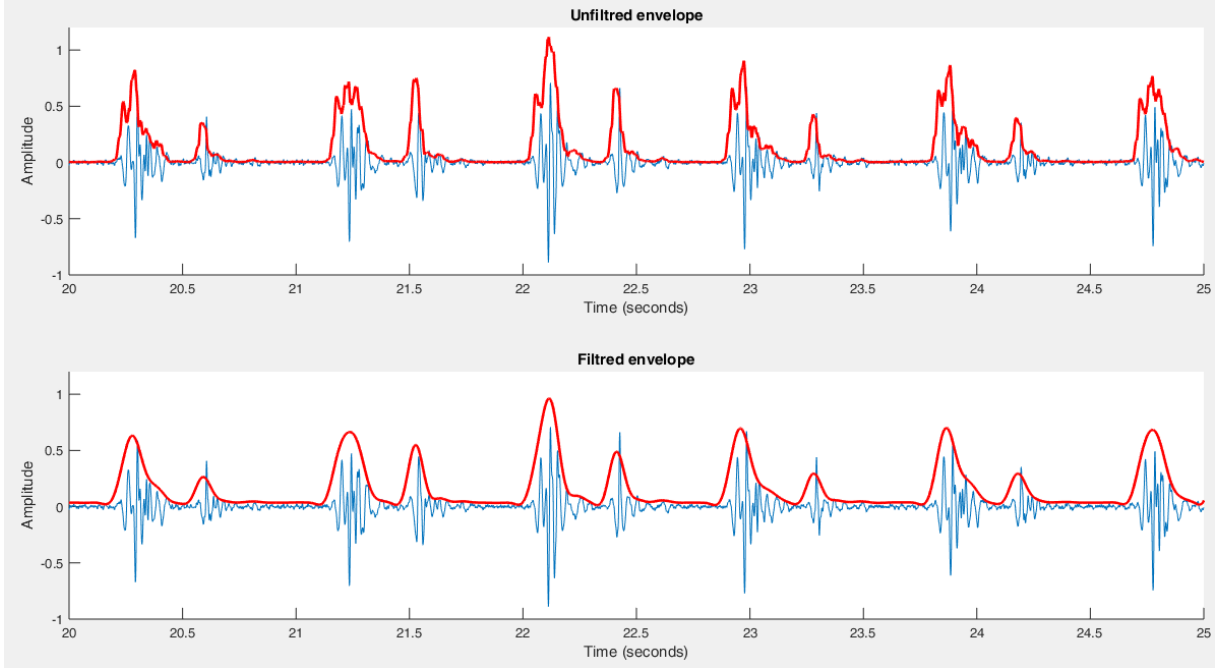


Figure 22: PCG - Envelope Filtration

3.4 ECG Processing

From the point of view of ECG and PCG synchronization, the R peak and the T wave are to be detected from the ECG signal.

3.4.1 R Peak Detection

The R peak of the QRS complex in ECG is determined to find the RR interval. For the detection of the QRS complex respectively the R peak detection, the edited Pan Tomkins algorithm [38] and the open source implementation of this algorithm for Matlab environment was used [39]. Block diagram of algorithm is shown on figure bellow.

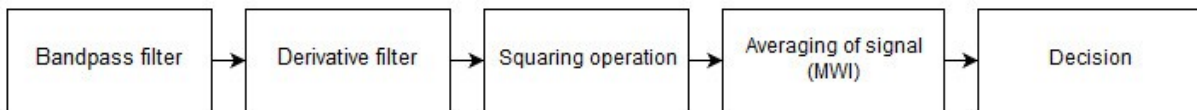


Figure 23: ECG - R Peak Detection - Block Diagram

Firstly, in order to attenuate noise the signal passes through a digital bandpass filter which passes frequencies in the range 8 - 20 Hz. This is an innovation from the original algorithm (which used the frequency range 5 - 15 Hz). According to Elgendi study [39] more accurate detection of QRS should be reached with the range 8 - 20 Hz. The next process after filtering is differentiation of the signal which provides information about the slope of the QRS complex. Differentiation is obtained by derivative filtration. Filtering is followed by squaring. The squaring process

intensifies the slope of the frequency response curve of the derivative and helps to restrict false positives caused by T waves with higher than usual spectral energies. After that the signal is averaged with a moving window (0.150 seconds length) to get rid of noise. The moving window integrator produces a signal that includes information about both the slope and the width of the QRS complex. The purpose of the moving-window integration is to obtain waveform feature information in addition to the slope of the R wave.

[39, 44]

At this point in the algorithm, the previous steps have generated a roughly pulse-shaped waveform at the output of the signal. The decision as to whether a pulse corresponds to a QRS complex (as opposed to a high-sloped T-wave or a noise artefact) is performed with an adaptive thresholding operation and other decision rules as a search back for QRS complexes, elimination of multiple detections within refractory period and T wave discrimination. The entire algorithm is described in detail in article of Pan and Tomkins [37] and Sedghamiz [38].

3.4.2 T Wave Detection

After determining the R peak, the search for the T wave peaks is relatively simple. The peak of the T wave in ECG is determined to find the RT interval. Block diagram of the T wave detection is shown below.

Most of the energy of T waves lies below 10 Hz [40, 41, 42]. With regard to this knowledge, the signal passes through a FIR Butterworth bandpass filter which passes frequencies in range 0.5 - 10 Hz. Then the signal is divided into individual RR segments obtained by the previous R peak detection.

In order to make T wave dominant feature in RR segments the QRS complexes are removed. The QRS duration is usually less than 100 milliseconds [43]. Therefore 50 ms at the start of RR segment and 50 ms at the end of segment are removed.

After the removal of the QRS complex local maxima are found in segments. For finding local maxima Matlab function *findpeaks()* was used. In leads I and II the amplitude should not be less than 0,05 mV [42]. In order to accomplish this minimal peak high is set. According to Gross [43] the duration of the T wave can be evaluated in relation to the cardiac cycle by the formula bellow.

$$T_{duration} = 0.08 + \frac{RR_{duration}}{10} \quad (5)$$

In order to this, minimal peak width for detection was set as 80% of $T_{duration}$ value.

The next step is only optional and enables to find the maximal value (and corresponding time) in the original ECG signal in a short time window (50 ms) around the peak of the T wave obtained in the previous steps. By the original ECG it is meant the ECG signal after removing iseline (frequencies bellow 0.5 Hz), notch filtering (50 Hz) and removing high frequency components (frequencies above 40 Hz).

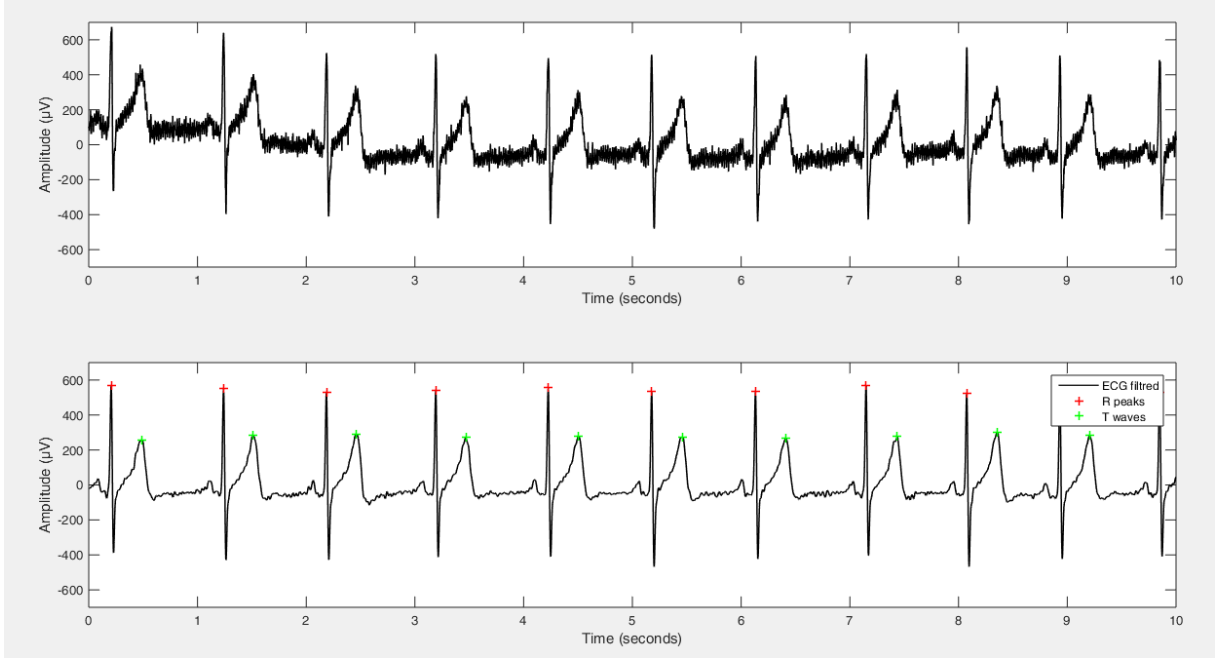


Figure 24: ECG Processing

3.4.3 Detection of S1 and S2

After extraction of the PCG signal envelope and determination of the R peak time and the T wave time, the first and the second heart sound can be estimated. The block diagram below describes the process of sound detection.

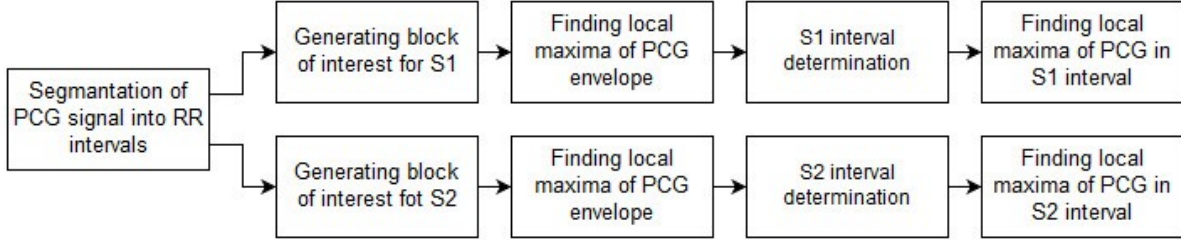


Figure 25: Heart Sound Detection - Block Diagram

Firstly, the PCG signal and its envelope is divided into segments bounded by the R peak. In these intervals, the first and the second heart sounds are later detected.

According to the clinical knowledge the first heart sound occurs always after the R peak and the second heart sound occurs with the end of the T wave for healthy heart conditions. It is difficult to determine the exact time of S1 or S2 interval. However, it is possible to get wider time blocks - blocks of interest, in which S1 and S2 are likely to be found. The time intervals for the blocks of interest were determined on the basis of the El-Segaier study [14]. In the study, they determine time intervals for S1 and S2 sound based on the RR and the RT interval where

the RR is time between adjacent R peaks and the RT interval is time between the R peak and the next peak of the T wave. According to this knowledge, the block of interest for S1 was determined as 0.05 RR to 0.2 RR and the block of interest for S2 was determined as 1.2 RT to 0.65 RR.

In the next steps, local maxima (using Matlab function `findpeaks()`) of the PCG envelope in both blocks of interest are found. The signal outside the block of interest is ignored for detection purpose. In case of no local maximum or many local maxima, the most significant peak in the block of interest is selected.

Neither S1 nor S2 sound are a single moment event. They are represented as an interval on the time axis. For comparison and later statistics there is necessary to have only one moment easily described and obtained for each sound. One of the ways how obtain this kind of time information is getting local maximum of the envelope, how to detect it is described above.

Another way can be detection of the maximal amplitude of the PCG signal (not the envelope). For that, firstly, the interval of sound has to be determined. The duration of sound was not obtained by defining the threshold to find the two boundaries for each sound. Since this way of detection may lead to inaccurate boundaries because of noise, murmurs etc.[15], in this work, the duration of sound set to the fixed value is based on clinical knowledge for each sound. This method can be also inaccurate because the duration varies with age, area of measuring and many other factors. [46] However, for purpose of detection we need only an approximate duration of sound. According to the previous study the duration of S1 sound was set to 145 ms and the duration of S2 was set to 110 ms [46]. In this window around S1 and S2 (S1 and S2 estimated as local maximum of the envelope), the maximum of PCG signal or maximum of absolute value of PCG signal can be found. These maximums can be taken as S1 and S2 sounds. The result of these three ways of detection are on the figure 26 bellow.

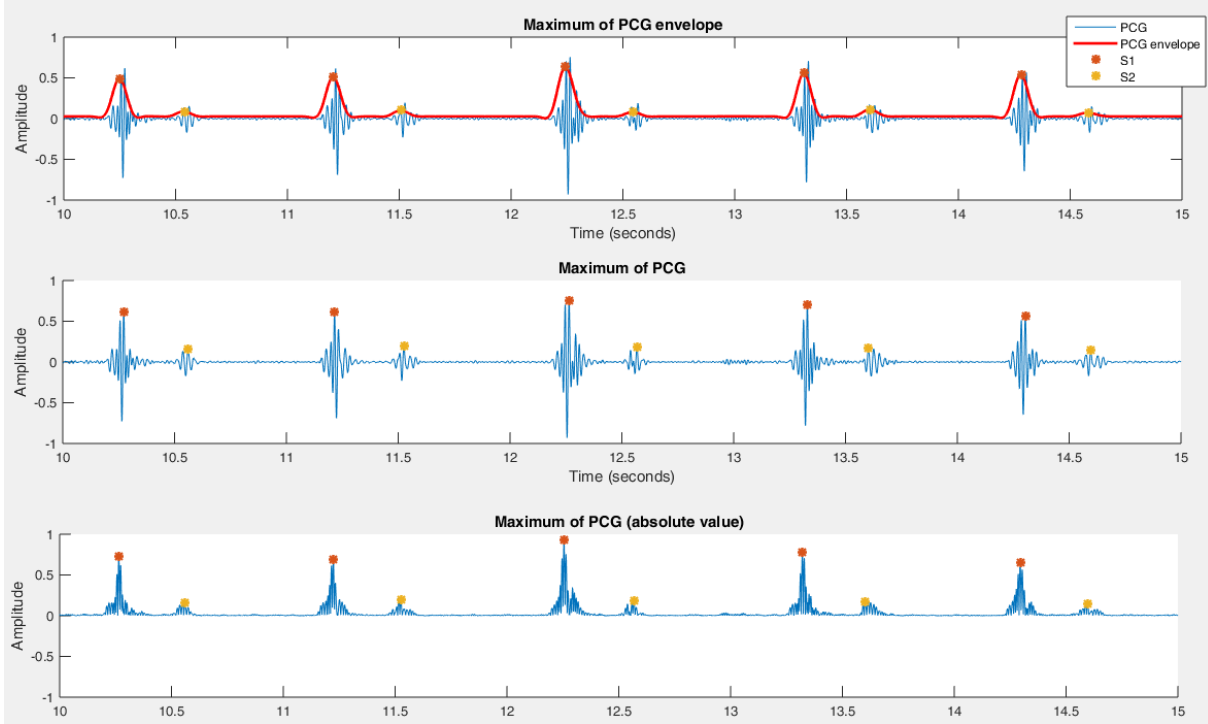


Figure 26: Different Ways Obtaining S1s and S2s

3.4.4 Calculation of Parameters

With determined heart sounds and R peaks and T waves on the ECG signal, different parameters necessary for the time domain analysis can be calculated. The calculated intervals include R - R, R - T, R - S1, R - S2, S1 - S1, S1 - S2, S2 - S2, their meaning is shown in the figure below. After detection, for each channel (position), seven vectors of data (intervals) are obtained.

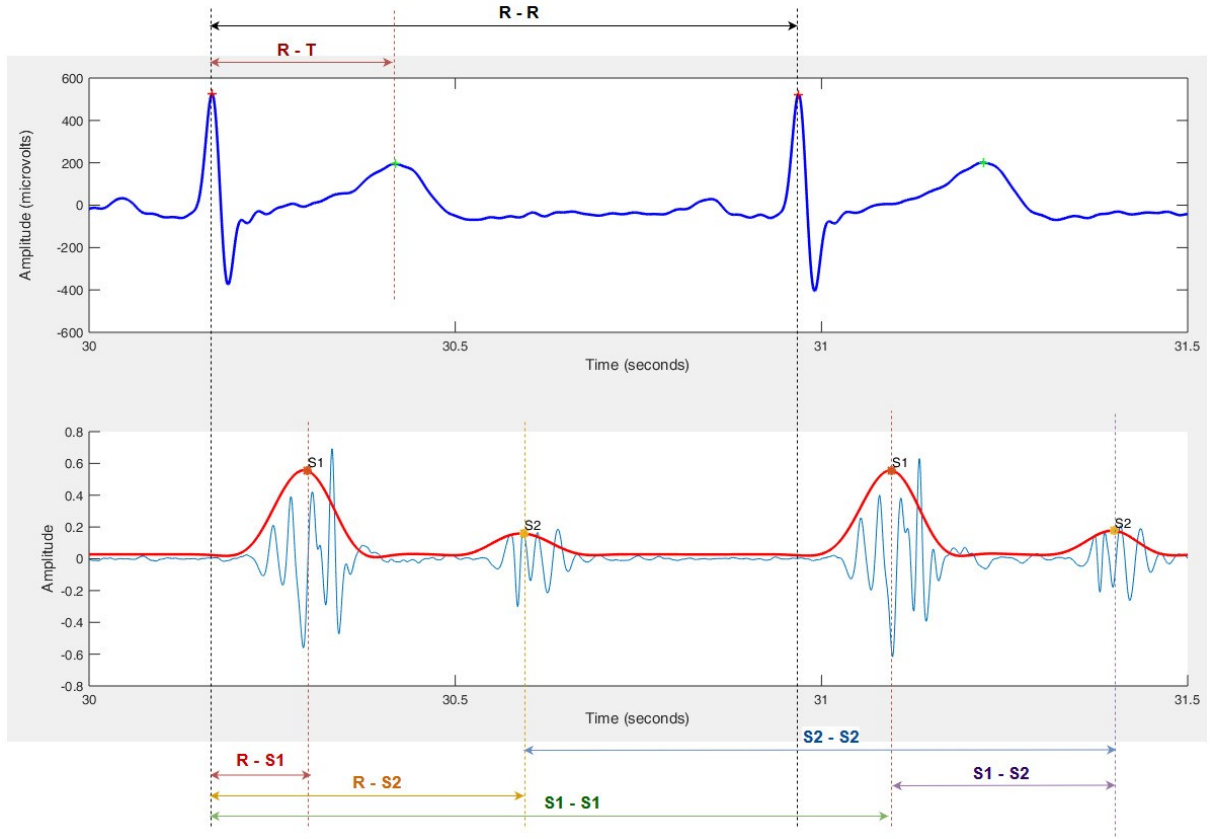


Figure 27: Examined Intervals

Computation of individual intervals is described in the table 5 below.

Table 5: Computation of the Intervals

Interval	Meaning	Calculation
R-R	The interval between two adjacent R peaks	$R - R = R_{x+1} - R_x$
R-T	The interval between R peak and next top of T wave	$R - T = T_x - R_x$
R-S1	The interval between R peak (ECG) and next S1 sound (PCG)	$R - S1 = S1_x - R_x$
R-S2	The interval between R peak (ECG) and next S2 sound (PCG)	$R - S2 = S2_x - R_x$
S1-S1	The interval between two adjacent S1 sounds	$S1 - S1 = S1_{x+1} - S1_x$
S2-S2	The interval between two adjacent S2 sounds	$S2 - S2 = S2_{x+1} - S2_x$
S1-S2	The interval between S1 sound and next S2 sound	$S1 - S2 = S2_x - S1_x$

4 Analysis of the Heart Sounds

More than 3 hours of both PCG and ECG signal were recorded during the work in more than 50 measurements. After detection of heart sounds and calculation of different intervals, time domain analysis can be performed. Different intervals were tested using statistical methods so that the differences between the signal measured from different positions are understandable.

4.1 R - R and S1 - S1 interval analysis

The analysis of the R - R interval to the S1 - S1 interval was performed because its results may provide information about relationship between ECG (as a reference signal) and PCG. The principle of the proposed detector suggests that the BPM calculated from ECG, where R spikes indicate the borders of each cardiac cycle, will be the same as the BPM calculated by the PCG signal, where the heart cycle boundaries are S1 sounds. However, BPM only gives the number of cardiac cycles per unit of time and says nothing about the length of each cardiac cycle. Therefore, in order to determine whether the length of cardiac cycles determined by ECG is the same as length of cardiac cycles determined by PCG, detailed analysis of R-R and S1 - S1 intervals and statistical testing is necessary. The results of this analysis can also confirm the functionality of the proposed detection algorithm. Analysed intervals are shown in the figure 28 below.

Due to the scale of the set of statistical outputs, only parts of the statistical results are shown in this text. Complete statistical results include exploratory data analysis (including boxplots, histograms, qq plots), normality tests results, confidence intervals and results from statistical hypothesis testing can be found in the Statistics appendix.

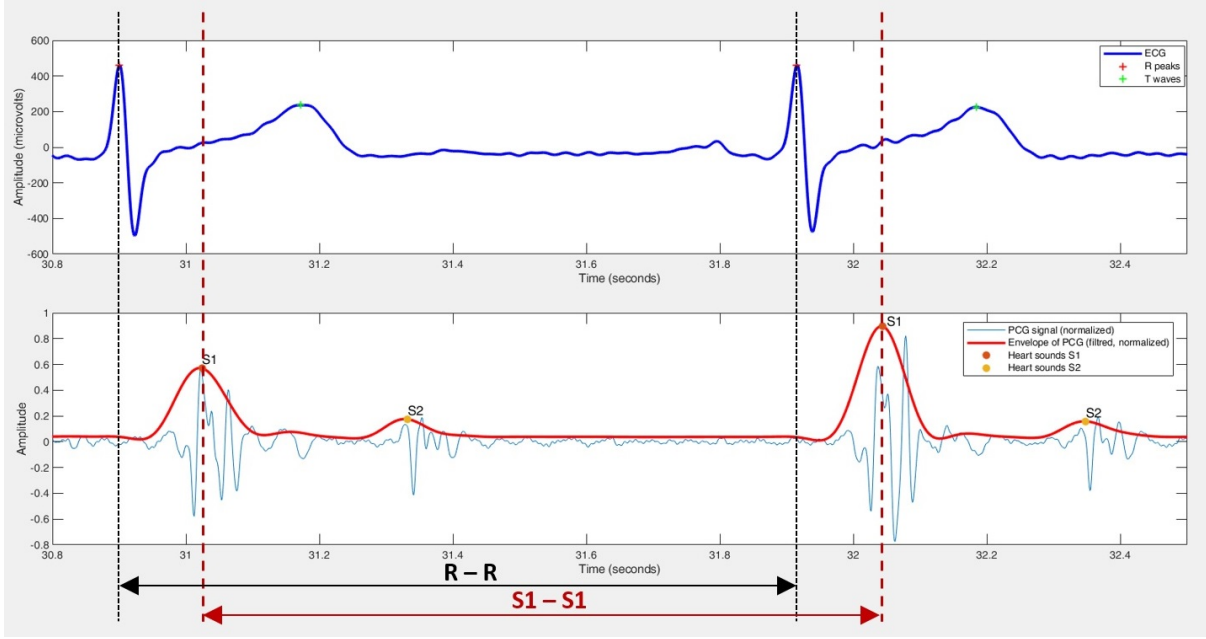


Figure 28: R - R and S1 - S1 Interval

4.1.1 Description of Data File

To analyse R - R interval in comparison with S1 - S1 interval, **7325 cardiac cycles** in total were measured using 12 PCG sensors and reference ECG. From these cycles, R - R intervals and S1 - S1 intervals were calculated and exported for further statistical computing in R programming language. Two different methods were used to calculate the S1 - S1 interval. The first used the maximum of the PCG signal envelope (S1 - S1) and the second used maximum of absolute value of the PCG signal (S1 Abs - S1 Abs) - see the chapter Detection of S1 and S2 3.4.3.

In the following paragraphs, the R - R and S - S interval analysis is performed for each **auscultation site** and each patient.

4.1.2 Auscultation Site A

Exploratory data analysis

In this paragraph only exploratory analysis outputs for one patient (and one method) are shown. Complete outputs (other patients and other detection methods) are attached in Statistics appendix.

Table 6: Auscultation Site A, Patient A: Duration of S1 - S1 (R - R) interval (ms)

Position of Sensor	IC2 R1	IC2 L1	IC2 L2	IC3 L1	IC3 L2	IC3 L3	IC4 L1	IC4 L2	IC4 L3	IC5 L1	IC5 L2	IC5 L3	RR
Count	1799	1799	1799	1799	1799	1799	1799	1799	1799	1799	1799	1799	1799
Minimum	758	784	772	784	730	770	780	782	754	768	770	752	785
Lower quartile	968,0	972,0	968,0	972,0	966,0	968,0	968,0	968,0	967,0	968,0	966,0	968,0	973,0
Average	1022,6	1022,4	1022,5	1022,4	1022,5	1022,5	1022,5	1022,4	1022,5	1022,5	1022,4	1022,5	1022,5
Median	1026,0	1028,0	1024,0	1028,0	1026,0	1026,0	1028,0	1028,0	1026,0	1026,0	1024,0	1024,0	1026,0
Upper quartile	1082,0	1080,0	1082,0	1078,0	1082,0	1080,0	1080,0	1082,0	1082,0	1083,0	1083,0	1082,0	1080,0
Maximum	1300	1232	1256	1240	1270	1238	1242	1242	1238	1236	1236	1248	1239
Standard deviation	83,6	78,9	84,0	78,3	83,4	80,9	80,6	82,5	83,3	80,9	83,6	81,1	78,5
Coeff. of variation (%)	8,2	7,7	8,2	7,7	8,2	7,9	7,9	8,1	8,1	7,9	8,2	7,9	7,7
Std. skewness	-0,271	-0,328	-0,253	-0,316	-0,179	-0,266	-0,280	-0,277	-0,288	-0,234	-0,184	-0,260	-0,314
Std. kurtosis	-0,096	-0,169	-0,105	-0,168	-0,254	-0,198	-0,200	-0,268	-0,066	-0,296	-0,291	-0,169	-0,200

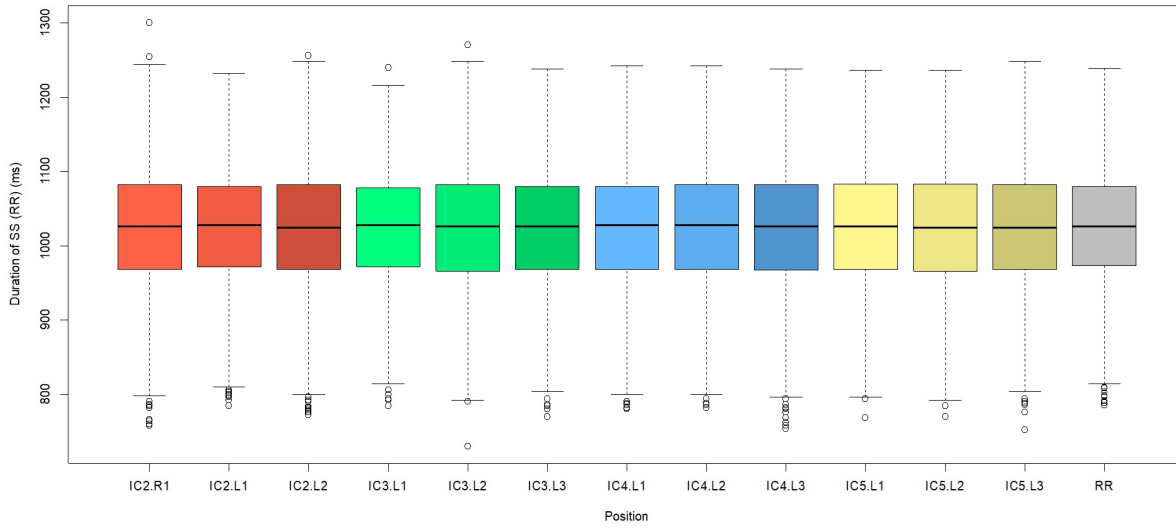


Figure 29: Duration of S1 - S1 (R - R) interval

Assessment of Normality

Normality tests were used to determine if a data set is well-modeled by a normal distribution. These tests were necessary for the selection of the method of statistical hypothesis testing.

- **Selected test:** Shapiro - Wilk Normality Test [50]
- **Null hypothesis H_0 :** Duration of intervals is normally distributed
- **Alternative hypothesis H_A :** $\neg H_0$
- **Results:**

At the significance level 0,05, it cannot be assumed normality of S1 – S1 intervals at any sensor position. Also it cannot be assumed normality of R - R interval. For further testing, tests requiring presumption of normality will be omitted.

The normality test results were the same for both patients tested. Also results were the same for S1 Abs - S1 Abs intervals.

Confidence Intervals

- **Estimated parameter:** $X_{0.5}$ (Median)

- **Results S1 – S1 intervals - patient A:**

Results in format $P(\text{Left Side (ms)} < X_{0.5} < \text{Right Side (ms)}) = 0,950$

Table 7: Auscultation Site A, Patient A: Confidence Intervals for Median of S1 - S1 Interval (ms)

Position of Sensor	Left Side	Right Side
IC2 R1	1021,0	1029,0
IC2 L1	1021,0	1029,0
IC2 L2	1020,0	1028,0
IC3 L1	1021,0	1029,0
IC3 L2	1020,0	1028,0
IC3 L3	1021,0	1028,0
IC4 L1	1021,0	1028,0
IC4 L2	1021,0	1029,0
IC4 L3	1021,0	1028,0
IC5 L1	1020,0	1028,0
IC5 L2	1020,0	1028,0
IC5 L3	1020,0	1028,0
RR	1021,0	1028,5

Table 8: Auscultation Site A, Patient A: Confidence Intervals for Median of S1 Abs - S1 Abs Interval (ms)

Position of Sensor	Left Side	Right Side
IC2 R1	1021,0	1029,5
IC2 L1	1020,5	1028,5
IC2 L2	1020,5	1029,0
IC3 L1	1021,0	1028,5
IC3 L2	1019,5	1028,0
IC3 L3	1020,5	1028,5
IC4 L1	1021,0	1028,5
IC4 L2	1021,0	1029,0
IC4 L3	1020,0	1028,5
IC5 L1	1021,0	1028,5
IC5 L2	1020,0	1028,0
IC5 L3	1019,5	1027,5
RR	1021,0	1028,5

Table 9: Auscultation Site A, Patient B: Confidence Intervals for Median of S1 - S1 Interval (ms)

Position of Sensor	Left Side	Right Side
IC2 R1	784,0	796,0
IC2 L1	784,0	796,0
IC2 L2	781,0	792,0
IC3 L1	781,0	791,0
IC3 L2	781,0	792,0
IC3 L3	782,0	792,0
IC4 L1	783,0	795,0
IC4 L2	781,0	792,0
IC4 L3	782,0	792,0
IC5 L1	782,0	792,0
IC5 L2	782,0	792,0
IC5 L3	782,0	792,0
RR	781,5	791,5

Table 10: Auscultation Site A, Patient B: Confidence Intervals for Median of S1 Abs - S1 Abs Interval (ms)

Position of Sensor	Left Side	Right Side
IC2 R1	784,0	798,5
IC2 L1	782,5	797,5
IC2 L2	780,5	792,0
IC3 L1	780,5	791,0
IC3 L2	780,5	791,5
IC3 L3	781,0	791,5
IC4 L1	782,0	795,5
IC4 L2	781,0	791,5
IC4 L3	781,5	792,0
IC5 L1	781,5	793,0
IC5 L2	781,5	792,0
IC5 L3	781,5	792,0
RR	781,5	791,5

Based on the selection, it can be, on level of certainty 95 % , assured that the medians of S1 - S1 intervals (S1 Abs – S1 Abs intervals) are within intervals between the boundaries given in the tables above.

Statistical Hypothesis Testing

This testing determines whether there are statistically significant differences in the duration of S1 - S1 intervals (S1 Abs - S1 Abs intervals) obtained from individual chest positions (and R - R interval).

- **Parameter tested:** $X_{0.5}$ (Median)
- **Selected test:** Friedman test [51, 52]
- H_0 : $X_{0.5 \text{ interval position IC2 R1}} = \dots = X_{0.5 \text{ interval position IC5 L3}} = X_{0.5 \text{ interval R R}}$
- H_A : $\neg H_0$
- **Test assumptions:**
 - There is one group of test subjects that are measured on three or more different occasions. ✓
 - The group is a random sample from the population. ✓
 - The dependent variable is at least an ordinal or continuous ✓
- **P - values:**

Table 11: Friedman Test: P - values

Tested Intervals	Patient	P - value
RR and S1 - S1	A	0,051
RR and S1 Abs - S1 Abs	A	0,840
RR and S1 - S1	B	0,995
RR and S1 Abs - S1 Abs	B	0,887

- **Results:**

For all tested intervals H_0 was not rejected at the 5% significance level. **The differences in the duration of the R - R and S1 - S1 intervals are not statistically significant.** (The differences in the duration of the R - R and S1 Abs - S1 Abs intervals are not statistically significant either).

Statistical Hypothesis Testing of S1 - S1 and S1 Abs - S1 Abs

This testing should determine whether there are statistically significant differences in the duration of the S1 - S1 and S1 Abs S1 intervals.

- **Parameter tested:** $X_{0.5}$ (Median)

- **Selected test:** Paired Samples Wilcoxon Test [53]
- H_0 : $X_{0.5 \text{ S1-S1 interval position A}} = X_{0.5 \text{ S1 Abs-S1 Abs interval position A}}$
- H_A : $\neg H_0$
- **Test assumptions:**
 - Data are paired and come from the same population . ✓
 - Each pair is chosen randomly and independently. ✓
 - The data are measured on at least an interval scale. ✓
- **P - values:**

Table 12: Auscultation Site A, Patient A: Paired Samples Wilcoxon Test: p - values

Position of Sensor	P - value
IC2 R1	0,798
IC2 L1	0,494
IC2 L2	0,891
IC3 L1	0,554
IC3 L2	0,635
IC3 L3	0,685
IC4 L1	0,263
IC4 L2	0,944
IC4 L3	0,902
IC5 L1	0,548
IC5 L2	0,789
IC5 L3	0,597

Table 13: Auscultation Site A, Patient B: Paired Samples Wilcoxon Test: p - values

Position of Sensor	P - value
IC2 R1	0,940
IC2 L1	0,805
IC2 L2	0,755
IC3 L1	0,959
IC3 L2	0,916
IC3 L3	0,745
IC4 L1	0,794
IC4 L2	0,758
IC4 L3	0,672
IC5 L1	0,989
IC5 L2	0,784
IC5 L3	0,693

- **Results:**

For all tested intervals H_0 was not rejected at the 5% significance level. **The differences in the duration of the S1 - S1 intervals and S1 Abs - S1 Abs intervals are not statistically significant at any of the positions on the chest.**

4.1.3 Auscultation Site B

Exploratory data analysis

In this paragraph only exploratory analysis outputs for one patient (and one method) are shown. Complete outputs (other patients and other detection methods) are attached in Statistics appendix.

Table 14: Auscultation Site B: Duration of S1 - S1 (R - R) Interval (ms)

Position of Sensor	IC2 R AORTIC	IC 2 L PULMONARY	IC4 L TRICUSPID	IC5 L MITRAL	RR
Count	3125	3125	3125	3125	3125
Minimum	694	640	704	652	699
Lower quartile	870,0	872,0	874,0	866,0	873,0
Average	938,6	938,6	938,6	938,7	938,6
Median	936,0	936,0	934,0	936,0	936,0
Upper quartile	1004,0	1002,0	1002,0	1008,0	1001,0
Maximum	1204	1202	1198	1206	1199
Standard deviaton	91,4	89,9	88,8	96,4	87,5
Coeff. of variation (%)	9,7	9,6	9,5	10,3	9,3
Stnd. skewness	0,131	0,119	0,155	0,129	0,155
Stnd. kurtosis	-0,563	-0,509	-0,559	-0,577	-0,554

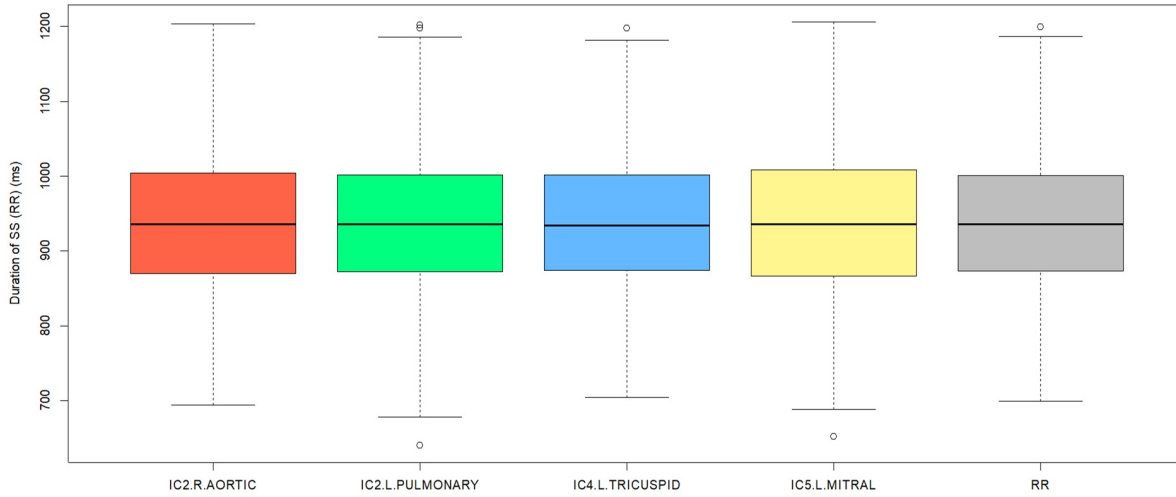


Figure 30: Duration of S1 - S1 (R - R) interval

Assessment of Normality

Normality tests were used to determine if a data set is well-modeled by a normal distribution. These tests were necessary for the selection of the method of statistical hypothesis testing.

- **Selected test:** Shapiro - Wilk Normality Test [50]
- **Null hypothesis H_0 :** Duration of intervals is normally distributed
- **Alternative hypothesis H_A :** $\neg H_0$

- **Results:**

At the significance level 0,05, it cannot be assumed normality of S1 – S1 intervals at any sensor position. Also it cannot be assumed normality of R - R interval. For further testing, tests requiring presumption of normality will be omitted.

The normality test results were the same for both patients tested. Also results were the same for S1 Abs - S1 Abs intervals.

Confidence Intervals

- **Estimated parameter:** $X_{0,5}$ (Median)

- **Results S1 – S1 intervals - patient A:**

Results In format $P(\text{Left Side (ms)} < X_{0,5} < \text{Right Side (ms)}) = 0,950$

Table 15: Auscultation Site B, Patient A: Confidence Intervals for Median of S1 - S1 Interval (ms)

Position of Sensor	Left Side	Right Side
IC2 R - AORTIC	934,0	941,0
IC2 L - PULMONARY	934,0	941,0
IC4 L - TRICUSPID	934,0	941,0
IC5 L - MITRAL	934,0	941,0
RR	934,0	940,5

Table 16: Auscultation Site B, Patient A: Confidence Intervals for Median of S1 Abs - S1 Abs Interval (ms)

Position of Sensor	Left Side	Right Side
IC2 R - AORTIC	934,0	941,0
IC2 L - PULMONARY	934,0	941,0
IC4 L - TRICUSPID	934,0	941,0
IC5 L - MITRAL	934,0	941,0
RR	934,0	940,5

Table 17: Auscultation Site B, Patient B: Confidence Intervals for Median of S1 - S1 Interval (ms)

Position of Sensor	Left Side	Right Side
IC2 R - AORTIC	955,0	964,0
IC2 L - PULMONARY	955,0	964,0
IC4 L - TRICUSPID	955,0	964,0
IC5 L - MITRAL	955,0	964,0
RR	955,0	964,0

Table 18: Auscultation Site B, Patient B: Confidence Intervals for Median of S1 Abs - S1 Abs Interval (ms)

Position of Sensor	Left Side	Right Side
IC2 R - AORTIC	955,5	964,5
IC2 L - PULMONARY	954,5	964,0
IC4 L - TRICUSPID	955,0	964,5
IC5 L - MITRAL	955,0	964,5
RR	955,0	964,0

Based on the selection, it can be, on level of certainty 95 % , assured that the medians of S1 - S1 intervals, respectively S1 Abs – S1 Abs intervals are within intervals between the boundaries given in the tables above.

Statistical Hypothesis Testing

This testing determines whether there are statistically significant differences in the duration of S1 - S1 intervals (S1 Abs - S1 Abs intervals) obtained from individual chest positions (and R - R interval).

- **Parameter tested:** $X_{0.5}$ (Median)
- **Selected test:** Friedman test [51, 52]
- H_0 : $X_{0.5 \text{ interval position AORTIC}} = \dots = X_{0.5 \text{ interval position MITRAL}} = X_{0.5 \text{ interval R R}}$
- H_A : $\neg H_0$
- **Test assumptions:**
 - There is one group of test subjects that are measured on three or more different occasions. ✓
 - The group is a random sample from the population. ✓

- The dependent variable is at least an ordinal or continuous ✓

- **P - values:**

Table 19: Friedman Test: P - values

Tested Intervals	Patient	P - value
RR and S1 - S1	A	0,232
RR and S1 Abs - S1 Abs	A	0,498
RR and S1 - S1	B	0,741
RR and S1 Abs - S1 Abs	B	0,270

- **Results:**

For all tested intervals H_0 was not rejected at the 5% significance level. **The differences in the duration of the R - R and S1 - S1 intervals are not statistically significant.** (The differences in the duration of the R - R and S1 Abs - S1 Abs intervals are not statistically significant either).

Statistical Hypothesis Testing of S1 - S1 and S1 Abs - S1 Abs

This testing should determine whether there are statistically significant differences in the duration of the S1 - S1 and S1 Abs S1 intervals

- **Parameter tested:** $X_{0.5}$ (Median)
- **Selected test:** Paired Samples Wilcoxon Test [53]
- H_0 : $X_{0.5} \text{ S1-S1 interval position A} = X_{0.5} \text{ S1 Abs-S1 Abs interval position A}$
- H_A : $\neg H_0$
- **Test assumptions:**
 - Data are paired and come from the same population . ✓
 - Each pair is chosen randomly and independently. ✓
 - The data are measured on at least an interval scale. ✓
- **P - values:**

Table 20: Auscultation Site B, Patient A: Paired Samples Wilcoxon Test: p - values

Position of Sensor	P - value
IC2 R - AORTIC	0,782
IC2 L - PULMONARY	0,858
IC4 L - TRICUSPID	0,166
IC5 L - MITRAL	0,457

Table 21: Auscultation Site B, Patient B: Paired Samples Wilcoxon Test: p - values

Position of Sensor	P - value
IC2 R - AORTIC	0,786
IC2 L - PULMONARY	0,930
IC4 L - TRICUSPID	0,889
IC5 L - MITRAL	0,393

- **Results:**

For all tested intervals H_0 was not rejected at the 5% significance level. **The differences in the duration of the S1 - S1 intervals and S1 Abs - S1 Abs intervals are not statistically significant at any of the positions on the chest.**

4.2 Testing between Measurements

As mentioned above (see chapter Data Acquisition 2.4), data acquisition was performed using at least 2 minute measurements (individual **sessions**). Thus many data files were created for one patient. The number of data files corresponded to the number of measurements with the patient. However, for the analysis of R - S1 interval (also R - S2 interval), only one large data file was needed to contain all patient data. Before data from individual measurements were combined, it was necessary to determine whether there were statistically significant differences between measurements.

Each position on the chest was analysed individually - group variables were individual sessions. An exploratory data analysis, a normality test, a Kruskal-Wallis Test test and a post hoc analysis were performed for each chest position. Methods for exploratory data analysis and normality tests were the same as in chapter above therefore it will not be described again. Complete results and outputs from testing between measurements are in Statistics appendix.

Statistical Hypothesis Testing

This testing should determine whether there are statistically significant differences in the duration of the R - S1 intervals (or R - S1 Abs intervals) on the specific position on the chest between individual sessions.

- **Parameter tested:** $X_{0.5}$ (Median)
- **Selected test:** Kruskal - Wallis Rank Sum Test [54]
- H_0 : $X_{0.5 \text{ R-S1 position A session } 1} = \dots = X_{0.5 \text{ R-S1 position A session } (n-1)} = X_{0.5 \text{ R-S1 position A session } n}$
where:
n = number of sessions
A = one of 12 (or 4) position one the chest
- H_A : $\neg H_0$
- **Test assumptions:**
 - Samples drawn from the population are random. ✓
 - The observations are independent of each other. ✓
 - The measurement scale for the dependent variable should be at least ordinal. ✓

- **P - values:**

The P - values for each position on the chest are stored in the Statistics appendix.

- **Results:**

For all tested intervals H_0 was rejected at the 5% significance level. It can be concluded that there are significant differences of R - S1 intervals between the sessions.

Post Hoc Analysis From the output of the Kruskal-Wallis test is known that there is a significant difference of R - S1 intervals between the sessions. To determine, which pairs of session is different, post hoc analysis is necessary.

Dunn's test of multiple comparisons using rank sums was used for post hoc analysis. [55]

- **P - values:**

P-values and p-values adjusted by bonferroni method are stored together with the Kruskal-Wallis test results in the Statistics appendix.

- **Results:**

If p - value $< 0,05$ it can be concluded that there are significant differences of R - S1 intervals between tested pair of sessions.

Same methods with same results were used for R - S1 Abs interval, R - S2 interval and R - S2 Abs interval.

4.2.1 Results of Testing

All the test and further post hoc analysis suggests , that there are statistically significant differences in tested intervals between individual sessions. For all tested intervals, at least one pair

of measurement session was always significantly different. These results met expectations, as the intervals compared are not from the same cardiac cycle (even they are from the same chest position of the patient). However, for the further analysis, it should be noted that there were statistically significant differences between individual measurement sessions.

4.3 R - S1 Interval Analysis

The analysis of the R - S1 interval is very important in this work as it determines whether the detected sounds at different positions on the chest come within the same heart cycle at the same time. A possible time shift between detection of S1 at different positions may provide more information about the relationship between electrical activity of the heart and S1 propagation. Analysed intervals are shown in the figure 31 below.

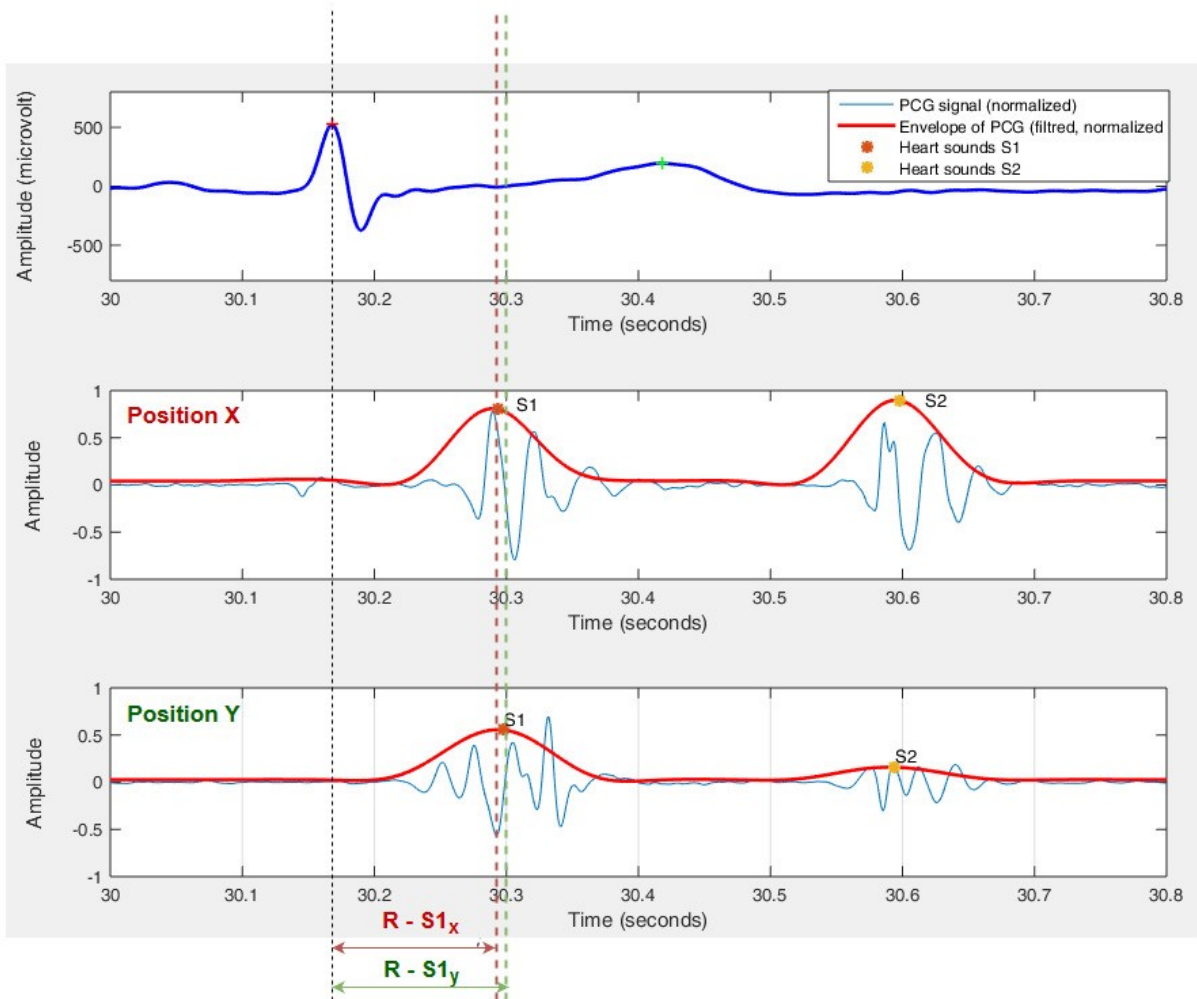


Figure 31: R - S1 Intervals

4.3.1 Description of Data File

To analyse R - S1 interval, respectively R - S1 Abs interval, **117 min** of 12 channel (or 4 channel) PCG record and reference ECG record were used. From this record, **7377** R - S1 (R - S1 Abs) intervals in total were calculated and exported for further statistical computing in R programming language. Two different methods were used to determine the R - S1 interval. The first one used the maximum of the PCG signal envelope as the first heart sound (R - S1) and the second one used sound maximum of absolute value of the PCG signal as the first heart sound (R - S1 Abs) - see the chapter Detection of S1 and S2 3.4.3.

In the following paragraphs, the R - S1 interval analysis is performed for different **auscultation sites**.

4.3.2 Auscultation Site A

In this paragraph only exploratory analysis outputs for one patient (and one method) are shown. Complete outputs (other patients and other detection methods) are attached in Statistics appendix.

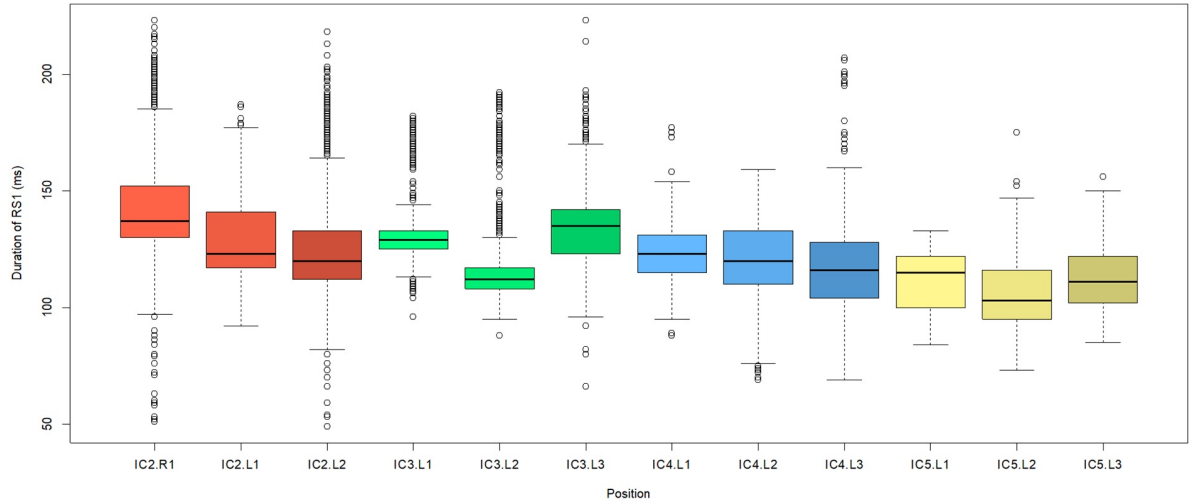


Figure 32: Auscultation site A, Patient A: Duration of R - S1 interval (ms)

Table 22: Auscultation Site A, Patient A: Duration of R - S1 interval (ms)

Position of Sensor	IC2 R1	IC2 L1	IC2 L2	IC3 L1	IC3 L2	IC3 L3	IC4 L1	IC4 L2	IC4 L3	IC5 L1	IC5 L2	IC5 L3
Count	1810	1810	1810	1810	1810	1810	1810	1810	1810	1810	1810	1810
Minimum	51	92	49	96	88	66	88	69	69	84	73	85
Lower quartile	130,0	117,0	112,0	125,0	108,0	123,0	115,0	110,0	104,0	100,0	95,0	102,0
Average	142,1	128,9	125,1	132,5	116,3	133,3	123,2	119,6	115,0	111,6	106,7	111,4
Median	137,0	123,0	120,0	129,0	112,0	135,0	123,0	120,0	116,0	115,0	103,0	111,0
Upper quartile	152,0	141,0	133,0	133,0	117,0	142,0	131,0	133,0	128,0	122,0	116,0	121,8
Maximum	223	187	218	182	192	223	177	159	207	133	175	156
Standard deviation	22,2	15,8	21,4	15,0	15,8	15,4	10,6	16,1	18,9	12,5	15,4	11,9
Coeff. of variation (%)	15,6	12,3	17,1	11,3	13,6	11,5	8,6	13,4	16,4	11,2	14,4	10,7
Std. skewness	0,490	0,903	1,089	1,873	2,892	0,392	0,341	-0,505	0,147	-0,476	0,704	0,106
Std. kurtosis	1,619	0,260	2,189	3,081	8,689	1,633	0,339	0,124	1,614	-1,125	-0,264	-0,826

Assessment of Normality

Normality tests were used to determine if a data set is well-modeled by a normal distribution. These tests were necessary for the selection of the method of statistical hypothesis testing.

- **Selected test:** Shapiro - Wilk Normality Test [50]
- **Null hypothesis H_0 :** Duration of intervals is normally distributed
- **Alternative hypothesis H_A :** $\neg H_0$
- **Results:**

At the significance level 0,05, it cannot be assumed normality of R – S1 intervals at any sensor position. For further testing, tests requiring presumption of normality will be omitted.

The normality test results were the same for both patients tested. Also results were the same for R - S1 Abs intervals.

Confidence Intervals

- **Estimated parameter:** $X_{0.5}$ (Median)
- **Results R – S1 intervals - patient A:**
Results in format $P(\text{Left Side (ms)} < X_{0.5} < \text{Right Side (ms)}) = 0,950$

Table 23: Auscultation Site A, Patient A: Confidence Intervals for Median of R - S1 Interval (ms)

Position of Sensor	Left Side	Right Side
IC2 R1	139,0	141,0
IC2 L1	127,0	129,0
IC2 L2	121,5	123,0
IC3 L1	129,0	129,5
IC3 L2	112,5	113,0
IC3 L3	132,5	134,0
IC4 L1	122,5	123,5
IC4 L2	120,0	121,5
IC4 L3	115,0	116,5
IC5 L1	111,0	112,5
IC5 L2	104,5	106,5
IC5 L3	111,0	112,0

Table 24: Auscultation Site A, Patient A: Confidence Intervals for Median of R - S1 Abs Interval (ms)

Position of Sensor	Left Side	Right Side
IC2 R1	155,0	158,5
IC2 L1	139,5	145,5
IC2 L2	137,5	139,5
IC3 L1	139,5	140,0
IC3 L2	120,0	120,5
IC3 L3	146,5	149,0
IC4 L1	135,0	136,0
IC4 L2	135,0	138,5
IC4 L3	127,0	128,5
IC5 L1	121,0	121,5
IC5 L2	115,5	118,5
IC5 L3	124,0	126,5

Table 25: Auscultation Site A, Patient B: Confidence Intervals for Median of R - S1 Interval (ms)

Position of Sensor	Left Side	Right Side
IC2 R1	121,5	126,5
IC2 L1	122,5	127,5
IC2 L2	122,5	124,5
IC3 L1	120,0	121,0
IC3 L2	122,5	123,5
IC3 L3	124,5	126,0
IC4 L1	128,5	131,5
IC4 L2	126,0	127,0
IC4 L3	122,0	124,0
IC5 L1	136,0	138,0
IC5 L2	142,0	143,0
IC5 L3	141,5	142,5

Table 26: Auscultation Site A, Patient B: Confidence Intervals for Median of R - S1 Abs Interval (ms)

Position of Sensor	Left Side	Right Side
IC2 R1	147,5	153,5
IC2 L1	149,0	154,5
IC2 L2	131,0	136,5
IC3 L1	126,5	128,0
IC3 L2	127,0	128,5
IC3 L3	130,5	131,5
IC4 L1	146,0	150,5
IC4 L2	137,0	139,0
IC4 L3	137,5	141,0
IC5 L1	153,5	158,5
IC5 L2	152,5	154,0
IC5 L3	151,5	153,0

Based on the selection, it can be, on level of certainty 95 % , assured that the medians of R - S1 intervals (R - S1 Abs intervals) are within intervals between the boundaries given in the tables above.

Statistical Hypothesis Testing

This testing determines whether there are statistically significant differences in the duration of R - S1 intervals (R - S1 Abs intervals) obtained from individual chest positions.

- **Parameter tested:** $X_{0.5}$ (Median)
- **Selected test:** Friedman test [51, 52]
- H_0 : $X_{0.5 \text{ interval position IC2 R1}} = \dots = X_{0.5 \text{ interval position IC5 L2}} = X_{0.5 \text{ interval position IC5 L3}}$
- H_A : $\neg H_0$
- **Test assumptions:**
 - There is one group of test subjects that are measured on three or more different occasions. ✓
 - The group is a random sample from the population. ✓
 - The dependent variable is at least an ordinal or continuous ✓
- **P - values:**

Table 27: Friedman test: P - values

Tested Intervals	Patient	P - value
R - S1	A	< 0,001
R - S1 Abs	A	< 0,001
R - S1	B	< 0,001
R - S1 Abs	B	< 0,001

- **Results:**

For all tested intervals H_0 was rejected at the 5% significance level. **The differences in the duration of the R - S1 intervals are statistically significant.**

Post Hoc Analysis

From the output of the Friedman test is known that there are significant differences of the R - S1 intervals between tested positions on the chest. To determine, which pairs of positions are different, post hoc analysis is necessary.

Friedman rank sum test with unreplicated blocked data was used for post hoc analysis. [56]

- **P - values:**

Due to the range of p - value tables for individual position pairs, **only pairs where the p - value is greater than or equal to 0,05 are displayed.** Complete tables with p - values are in the Statistics appendix.

Table 28: Auscultation Site A, Patient A, R - S1 Interval: P - Values from Post Hoc Analysis

Position Pair	P - Value
IC2 L1 - IC4 L1	0,070
IC2 L2 - IC4 L1	0,951
IC3 L2 - IC4 L3	0,068
IC5 L1 - IC5 L3	0,993

Table 29: Auscultation Site A, Patient A, R - S1 Abs Interval: P - Values from Post Hoc Analysis

Position Pair	P - Value
IC2 L1 - IC2 L2	0,073
IC2 L1 - IC4 L1	0,127
IC2 L1 - IC4 L2	0,157
IC3 L1 - IC3 L3	1,000
IC3 L2 - IC5 L3	0,986
IC4 L1 - IC4 L2	1,000
IC5 L1 - IC5 L3	0,105

Table 30: Auscultation Site A, Patient B, R - S1 Interval: P - Values from Post Hoc Analysis

Position Pair	P - Value
IC2 R1 - IC2 L1	1,000
IC2 R1 - IC3 L3	0,086
IC2 R1 - IC4 L2	1,000
IC2 L1 - IC3 L3	0,135
IC2 L1 - IC4 L2	1,000
IC2 L2 - IC3 L2	0,592
IC2 L2 - IC3 L3	0,984
IC2 L2 - IC4 L3	0,990
IC3 L2 - IC4 L3	0,999
IC3 L3 - IC4 L2	0,477
IC3 L2 - IC4 L3	0,374
IC5 L2 - IC5 L3	1,000

Table 31: Auscultation Site A, Patient B, R - S1 Abs Interval: P - Values from Post Hoc Analysis

Position Pair	P - Value
IC2 R1 - IC2 L1	1,000
IC2 R1 - IC4 L1	0,920
IC2 L1 - IC4 L1	0,917
IC2 L2 - IC3 L3	0,816
IC3 L1 - IC3 L2	1,000
IC4 L2 - IC4 L3	0,999
IC5 L1 - IC5 L2	0,968
IC5 L1 - IC5 L3	0,405
IC5 L2 - IC5 L3	0,997

- **Results:**

For the most of tested pairs (66 position pairs in total) are differences of R - S1 intervals (R - S1 abs intervals) at the 5% significance level statistically important. Duration of R - S1 intervals (R - S1 Abs intervals) is the same only for the positions mentioned in the tables above. However, since there is no match between these position pairs for different patients and different detection methods, it can be assumed that the **duration of the R - S1 interval (R - S1 Abs interval) is dependent on the position of the sensor.**

4.3.3 Auscultation Site B

In this paragraph only exploratory analysis outputs for one patient (and one method) are shown. Complete outputs (other patients and other detection methods) are attached in Statistics appendix.

Table 32: Auscultation Site B, Patient A: Duration of R - S1 interval (ms)

Position of Sensor	IC2 R AORTIC	IC2 L PULMONARY	IC4 L TRICUSPID	IC5 L MITRAL
Count	3149	3149	3149	3149
Minimum	40	38	96	44
Lower quartile	129,0	123,0	122,0	86,0
Average	138,0	131,1	127,4	106,5
Median	136,0	130,0	127,0	105,0
Upper quartile	147,0	138,0	132,0	123,0
Maximum	205	194	190	176
Standard deviaton	14,4	12,9	7,9	22,5
Coeff. of variance (%)	10,5	9,8	6,2	21,1
Stnd. skewness	0,034	0,175	0,644	0,357
Stnd. kurtosis	4,293	4,129	2,569	-0,833

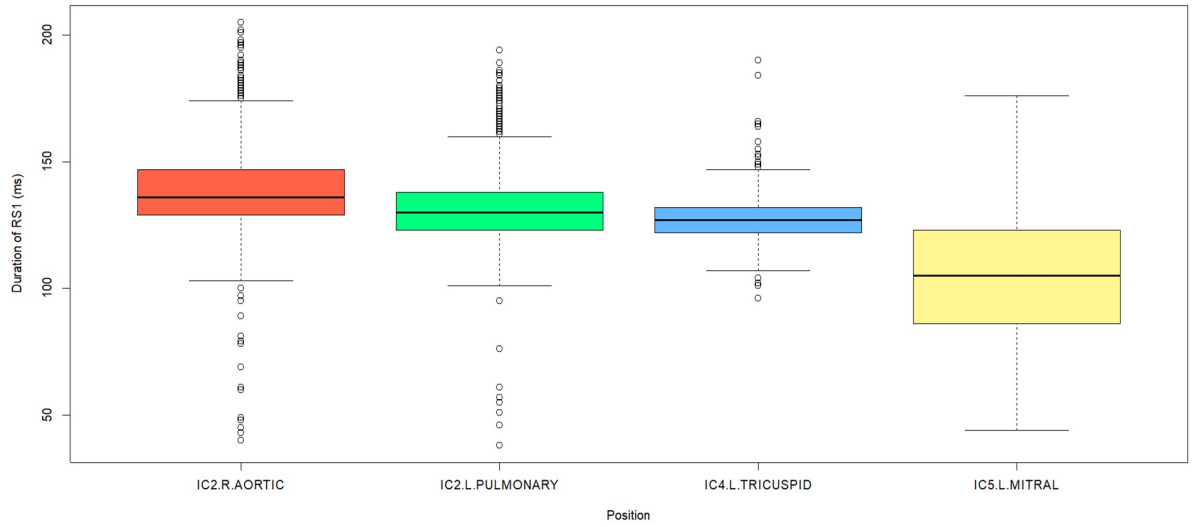


Figure 33: Auscultation site B, Patient A: Duration of R - S1 interval (ms)

Assessment of Normality

Normality tests were used to determine if a data set is well-modeled by a normal distribution. These tests were necessary for the selection of the method of statistical hypothesis testing.

- **Selected test:** Shapiro - Wilk Normality Test [50]
- **Null hypothesis H_0 :** Duration of intervals is normally distributed
- **Alternative hypothesis H_A :** $\neg H_0$
- **Results:**

At the significance level 0,05, it cannot be assumed normality of R – S1 intervals at any sensor position. For further testing, tests requiring presumption of normality will be omitted.

The normality test results were the same for both patients tested. Also results were the same for R - S1 Abs intervals.

Confidence Intervals

- **Estimated parameter:** $X_{0,5}$ (Median)
- **Results R – S1 intervals - patient A:**
Results in format $P(\text{Left Side (ms)} < X_{0,5} < \text{Right Side (ms)}) = 0,950$

Table 33: Auscultation Site B, Patient A: Confidence Intervals for Median of R - S1 Interval (ms)

Position of Sensor	Left Side	Right Side
IC2 R - AORTIC	137,0	138,0
IC2 L - PULMONARY	130,0	131,0
IC4 L - TRICUSPID	127,0	127,5
IC5 L - MITRAL	105,0	106,5

Table 34: Auscultation Site B, Patient A: Confidence Intervals for Median of R - S1 Abs Interval (ms)

Position of Sensor	Left Side	Right Side
IC2 R - AORTIC	149,5	151,0
IC2 L - PULMONARY	141,5	143,5
IC4 L - TRICUSPID	139,5	141,0
IC5 L - MITRAL	121,5	125,0

Table 35: Auscultation Site B, Patient B: Confidence Intervals for Median of R - S1 Interval (ms)

Position of Sensor	Left Side	Right Side
IC2 R - AORTIC	108,0	109,0
IC2 L - PULMONARY	115,5	117,0
IC4 L - TRICUSPID	105,0	106,0
IC5 L - MITRAL	114,5	115,0

Table 36: Auscultation Site B, Patient B: Confidence Intervals for Median of R - S1 Abs Interval (ms)

Position of Sensor	Left Side	Right Side
IC2 R - AORTIC	116,5	118,0
IC2 L - PULMONARY	124,5	126,5
IC4 L - TRICUSPID	108,5	109,5
IC5 L - MITRAL	128,0	129,0

Based on the selection, it can be, on level of certainty 95 % , assured that the medians of R - S1 intervals, respectively R – S1 Abs intervals are within intervals between the boundaries given in the tables above.

Statistical Hypothesis Testing

This testing determines whether there are statistically significant differences in the duration of R - S1 intervals (R - S1 Abs intervals) obtained from individual chest positions.

- **Parameter tested:** $X_{0.5}$ (Median)
- **Selected test:** Friedman test [51, 52]
- H_0 : $X_{0.5 \text{ interval position AORTIC}} = \dots = X_{0.5 \text{ interval position TRICUSPID}} = X_{0.5 \text{ interval position MITRAL}}$
- H_A : $\neg H_0$
- **Test assumptions:**
 - There is one group of test subjects that are measured on three or more different occasions. ✓
 - The group is a random sample from the population. ✓
 - The dependent variable is at least an ordinal or continuous ✓
- **P - values:**

Table 37: Friedman Test: P - values

Tested Intervals	Patient	P - value
R - S1	A	< 0,001
R - S1 Abs	A	< 0,001
R - S1	B	< 0,001
R - S1 Abs	B	< 0,001

- **Results:**

For all tested intervals H_0 was rejected at the 5% significance level. **The differences in the duration of the R - S1 intervals are statistically significant.**

Post Hoc Analysis

From the output of the Friedman test, is known that there are significant differences of R - S1 intervals between tested positions on the chest. To determine, which pairs of positions are different, post hoc analysis is necessary.

Friedman rank sum test with unreplicated blocked data was used for analysis. [56]

- **P - values:**

All p - values were less than 0,001. Complete tables with p - values are in the Statistics appendix.

- **Results:**

For all tested positions were differences of R - S1 intervals (R - S1 Abs intervals) at the 5% significance level statistically important. It can be assumed that the **duration of the R - S1 interval (R - S1 Abs interval) is dependent on the position of the sensor.**

4.4 R - S2 Interval Analysis

As in the case of R - S1 analysis, also analysis of the R - S2 interval is very important in this work. R - S2 analysis determines whether the detected sounds at different positions on the chest come within the same heart cycle at the same time. A possible time shift between detection of S2 at different positions may provide more information about the relationship between electrical activity of the heart and S2 propagation. Analysed intervals are shown in the figure 34 below.

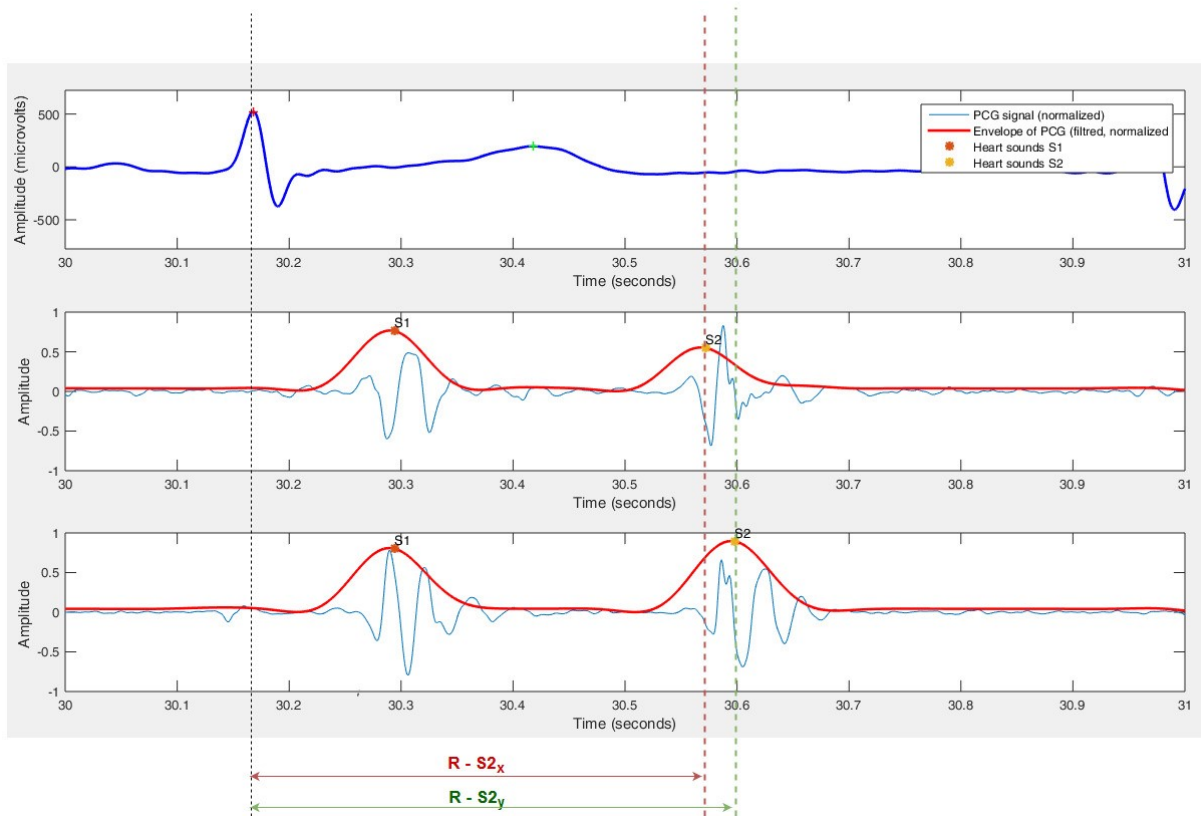


Figure 34: R - S2 Intervals

4.4.1 Description of Data File

To analyse R - S2 interval, respectively R - S2 Abs interval, **117 min** of 12 channel (or 4 channel) PCG record and reference ECG record were used. From this record, **7377** R - S2 (R - S2 Abs) intervals in total were calculated and exported for further statistical computing in R programming language. Two different methods were used to determine the R - S2 interval.

The first one used the maximum of the PCG signal envelope as the second heart sound (R – S2) and the second one used maximum of absolute value of the PCG signal as the second heart sound (R – S2 Abs) - see the chapter Detection of S1 and S2 3.4.3.

In the following paragraphs, the R - S2 interval analysis is performed for different **auscultation sites**.

4.4.2 Auscultation Site A

In this paragraph only exploratory analysis outputs for one patient (and one method) are shown. Complete outputs (other patients and other detection methods) are attached in Statistics appendix.

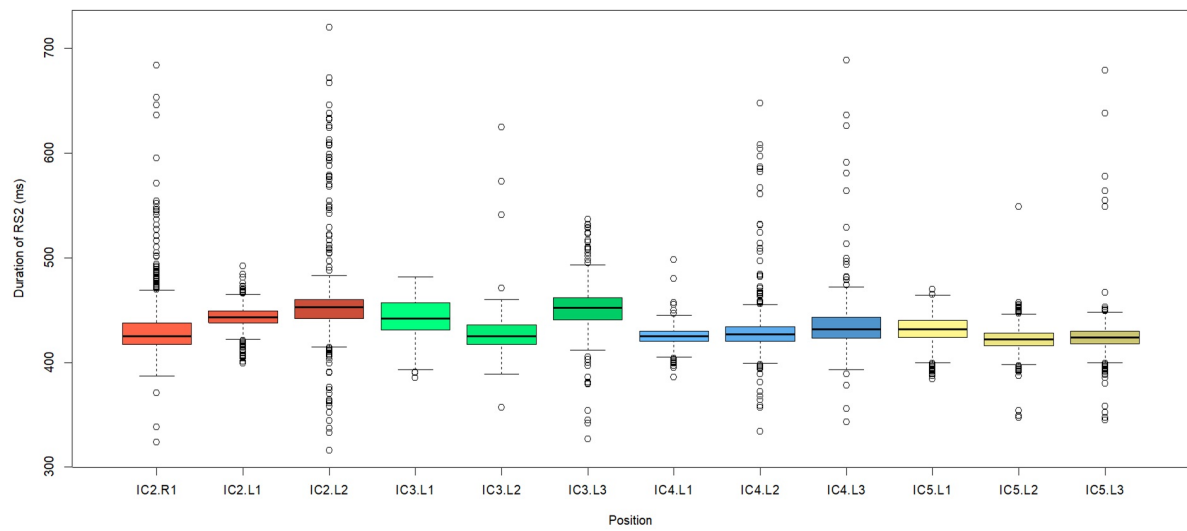


Figure 35: Auscultation Site A, Patient A: Duration of R - S2 interval (ms)

Table 38: Auscultation Site A, Patient A: Duration of R - S2 Interval (ms)

Position of Sensor	IC2 R1	IC2 L1	IC2 L2	IC3 L1	IC3 L2	IC3 L3	IC4 L1	IC4 L2	IC4 L3	IC5 L1	IC5 L2	IC5 L3
Count	1810	1810	1810	1810	1810	1810	1810	1810	1810	1810	1810	1810
Minimum	324	399	316	385	357	327	386	334	343	384	347	345
Lower quartile	417,0	438,0	442,0	431,0	417,0	441,0	420,0	420,0	423,0	424,0	416,0	418,0
Average	430,0	442,9	451,9	443,3	426,4	451,7	424,4	428,4	433,3	431,6	422,2	424,4
Median	425,0	443,0	453,0	442,0	425,0	452,0	425,0	427,0	432,0	432,0	422,0	424,0
Upper quartile	438,0	449,0	460,0	457,0	436,0	461,8	430,0	434,0	443,0	439,8	428,0	430,0
Maximum	684	492	720	482	625	537	498	648	689	470	549	679
Standard deviation	24,1	9,8	26,9	16,4	14,7	17,6	8,4	18,1	18,1	13,3	11,2	14,3
Coeff. of variance (%)	5,6	2,2	6,0	3,7	3,5	3,9	2,0	4,2	4,2	3,1	2,6	3,4
Stand. skewness	3,154	-0,178	3,258	-0,020	2,190	-0,088	0,146	4,368	3,936	-0,174	0,459	6,531
Stand. kurtosis	22,055	1,728	24,316	-0,603	24,705	5,260	4,778	40,757	44,345	0,450	11,718	101,756

Assessment of Normality

Normality tests were used to determine if a data set is well-modeled by a normal distribution. These tests were necessary for the selection of the method of statistical hypothesis testing.

- **Selected test:** Shapiro - Wilk Normality Test [50]
- **Null hypothesis H_0 :** Duration of intervals is normally distributed
- **Alternative hypothesis H_A :** $\neg H_0$
- **Results:**

At the significance level 0,05, it cannot be assumed normality of R – S2 intervals at any sensor position. For further testing, tests requiring presumption of normality will be omitted.

The normality test results were the same for both patients tested. Also results were the same for R - S2 Abs intervals.

Confidence Intervals

- **Estimated parameter:** $X_{0.5}$ (Median)
- **Results R – S2 intervals - patient A:**
Results in format $P(\text{Left Side (ms)} < X_{0.5} < \text{Right Side (ms)}) = 0,950$

Table 39: Auscultation Site A, Patient A: Confidence Intervals for Median of R - S2 Interval (ms)

Position of Sensor	Left Side	Right Side
IC2 R1	426,0	427,5
IC2 L1	442,5	443,5
IC2 L2	450,5	452,0
IC3 L1	442,5	444,0
IC3 L2	425,5	426,5
IC3 L3	450,5	452,0
IC4 L1	424,0	425,0
IC4 L2	427,0	428,0
IC4 L3	432,0	433,0
IC5 L1	431,0	432,5
IC5 L2	421,5	422,5
IC5 L3	423,5	424,5

Table 40: Auscultation Site A, Patient A: Confidence Intervals for Median of R - S2 Abs Interval (ms)

Position of Sensor	Left Side	Right Side
IC2 R1	435,0	436,0
IC2 L1	448,5	450,0
IC2 L2	460,5	463,0
IC3 L1	458,5	462,0
IC3 L2	432,0	433,5
IC3 L3	468,0	471,0
IC4 L1	438,0	439,5
IC4 L2	435,5	438,0
IC4 L3	426,5	427,5
IC5 L1	439,0	441,0
IC5 L2	426,0	426,5
IC5 L3	425,5	426,5

Table 41: Auscultation Site A, Patient B: Confidence Intervals for Median of R - S2 Interval (ms)

Position of Sensor	Left Side	Right Side
IC2 R1	430,5	433,0
IC2 L1	428,5	431,5
IC2 L2	437,5	439,0
IC3 L1	428,5	430,0
IC3 L2	434,0	435,5
IC3 L3	440,5	443,0
IC4 L1	427,5	430,5
IC4 L2	446,5	449,0
IC4 L3	445,0	447,5
IC5 L1	432,0	433,0
IC5 L2	445,5	447,5
IC5 L3	449,0	452,0

Table 42: Auscultation Site A, Patient B: Confidence Intervals for Median of R - S2 Abs Interval (ms)

Position of Sensor	Left Side	Right Side
IC2 R1	440,5	442,5
IC2 L1	439,5	441,5
IC2 L2	448,5	451,5
IC3 L1	441,0	442,0
IC3 L2	443,0	444,0
IC3 L3	458,0	462,5
IC4 L1	437,5	439,5
IC4 L2	458,0	461,5
IC4 L3	456,5	459,0
IC5 L1	441,5	442,5
IC5 L2	449,0	450,5
IC5 L3	434,5	436,5

Based on the selection, it can be, on level of certainty 95 % , assured that the medians of R - S2 intervals (R - S2 Abs intervals) are within intervals between the boundaries given in the tables above.

Statistical Hypothesis Testing

This testing determines whether there are statistically significant differences in the duration of R - S2 intervals (R - S2 Abs intervals) obtained from individual chest positions.

- **Parameter tested:** $X_{0.5}$ (Median)
- **Selected test:** Friedman test [51, 52]
- H_0 : $X_{0.5}$ interval position IC2 R1 = ... = $X_{0.5}$ interval position IC5 L2 = $X_{0.5}$ interval position IC5 L3
- H_A : $\neg H_0$
- **Test assumptions:**
 - There is one group of test subjects that are measured on three or more different occasions. ✓
 - The group is a random sample from the population. ✓
 - The dependent variable is at least an ordinal or continuous ✓
- **P - values:**

Table 43: Friedman Test: P - values

Tested Intervals	Patient	P - value
R - S1	A	< 0,001
R - S1 Abs	A	< 0,001
R - S1	B	< 0,001
R - S1 Abs	B	< 0,001

- **Results:**

For all tested intervals H_0 was rejected at the 5% significance level. **Differences in the duration of the R - S2 intervals are statistically significant.**

Post Hoc Analysis

From the output of the Friedman test, is known that there are significant differences of R - S2 intervals between tested positions on the chest. To determine, which pairs of positions is different, post hoc analysis is necessary.

Friedman rank sum test with unreplicated blocked data was used for post hoc analysis. [56]

- **P - values:**

Due to the range of p - value tables for individual position pairs, **only pairs where the p - value is greater than or equal to 0,05 are displayed.** Complete tables with p - values are in the Statistics appendix.

Table 44: Patient A, R - S2 interval: P - Values from Post Hoc Analysis

Position pair	p - value
IC2 R1 - IC4 L2	0,860
IC2 L2 - IC3 L3	0,996
IC3 L2 - IC4 L1	1,000
IC3 L2 - IC5 L3	0,999
IC4 L1 - IC5 L3	1,000
IC4 L3 - IC5 L1	0,866

Table 45: Patient A, R - S2 Abs interval: P - Values from Post Hoc Analysis

Position pair	p - value
IC2 R1 - IC4 L1	1,000
IC2 L1 - IC3 L1	0,983
IC2 L2 - IC3 L3	1,000
IC4 L2 - IC5 L1	0,901
IC5 L2 - IC5 L3	0,114

Table 46: Patient B, R - S2 interval: P - Values from Post Hoc Analysis

Position pair	p - value
IC2 R1 - IC2 L1	0,856
IC2 R1 - IC3 L2	0,333
IC2 R1 - IC4 L1	0,229
IC2 R1 - IC5 L1	0,758
IC2 L1 - IC4 L1	0,998
IC2 L1 - IC5 L1	1,000
IC2 L2 - IC3 L3	0,864
IC4 L1 - IC5 L1	1,000
IC4 L2 - IC4 L3	0,735
IC4 L2 - IC5 L2	0,998
IC4 L2 - IC5 L3	1,000
IC4 L3 - IC5 L2	0,135
IC4 L3 - IC5 L3	0,632
IC5 L2 - IC5 L3	1,000

Table 47: Patient B, R - S2 Abs interval: P - Values from Post Hoc Analysis

Position Pair	P - value
IC2 R1 - IC2 L1	0,966
IC2 R1 - IC3 L1	1,000
IC2 L1 - IC3 L1	0,939
IC2 L2 - IC3 L2	0,275
IC2 L2 - IC4 L2	0,144
IC3 L2 - IC4 L3	0,537
IC3 L2 - IC5 L1	0,249
IC3 L3 - IC4 L2	1,000
IC3 L3 - IC5 L2	0,762
IC4 L1 - IC5 L3	0,997
IC4 L2 - IC5 L2	0,905

- **Results:**

For the most of tested pairs (66 position pairs in total) are differences of R - S2 intervals (R - S2 abs intervals) at the 5% significance level statistically important. Duration of R - S2 intervals (R - S2 Abs intervals) is the same only for positions mentioned in tables above. However, since there is no match between these position pairs for different patients and different detection methods, it can be assumed that the **duration of the R - S2 (R - S2 Abs) interval is dependent on the position of the sensor.**

4.4.3 Auscultation site B

In this paragraph only exploratory analysis outputs for one patient (and one method) are shown. Complete outputs (other patients and other detection methods) are attached in Statistics appendix.

Table 48: Auscultation Site B, Patient A: Duration of R - S2 interval (ms)

Position of Sensor	IC2 R AORTIC	IC2 L PULMONARY	IC4 L TRICUSPID	IC5 L MITRAL
Count	3149	3149	3149	3149
Minimum	323	382	318	331
Lower quartile	414,0	432,0	420,0	413,0
Average	425,1	441,5	428,5	421,9
Median	422,0	442,0	428,0	420,0
Upper quartile	433,0	450,0	436,0	429,0
Maximum	531	626	623	691
Standard deviaton	17,1	15,8	14,0	18,8
Coeff. of variance (%)	4,0	3,6	3,3	4,5
Stnd. skewness	0,566	1,040	1,271	4,761
Stnd. kurtosis	0,834	9,490	20,710	50,546

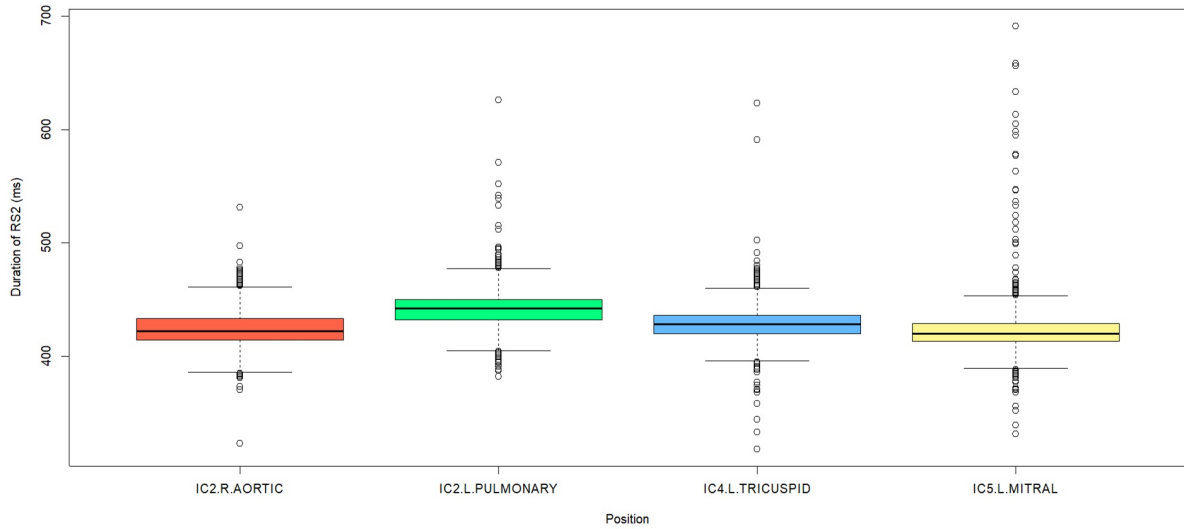


Figure 36: Auscultation Site B, Patient A: Duration of R - S2 interval (ms)

Assessment of Normality

Normality tests were used to determine if a data set is well-modeled by a normal distribution. These tests were necessary for the selection of the method of statistical hypothesis testing.

- **Selected test:** Shapiro - Wilk Normality Test [50]
- **Null hypothesis H_0 :** Duration of intervals is normally distributed
- **Alternative hypothesis H_A :** $\neg H_0$

- **Results:**

At the significance level 0,05, it cannot be assumed normality of R – S2 intervals at any sensor position. For the further testing, tests requiring presumption of normality will be omitted.

The normality test results were the same for both patients tested. Also results were the same for R - S2 Abs intervals.

Confidence Intervals

- **Estimated parameter:** $X_{0,5}$ (Median)

- **Results R – S2 intervals - patient A:**

Results in format $P(\text{Left Side (ms)} < X_{0,5} < \text{Right Side (ms)}) = 0,950$

Table 49: Auscultation Site B, Patient A: Confidence Intervals for Median of R - S2 Interval (ms)

Position of Sensor	Left Side	Right Side
IC2 R - AORTIC	423,0	424,5
IC2 L - PULMONARY	441,0	442,0
IC4 L - TRICUSPID	427,5	428,5
IC5 L - MITRAL	420,5	421,0

Table 50: Auscultation Site B, Patient A: Confidence Intervals for Median of R - S2 Abs Interval (ms)

Position of Sensor	Left Side	Right Side
IC2 R - AORTIC	434,0	434,5
IC2 L - PULMONARY	444,0	446,0
IC4 L - TRICUSPID	437,0	438,5
IC5 L - MITRAL	428,0	429,0

Table 51: Auscultation Site B, Patient B: Confidence Intervals for Median of R - S2 Interval (ms)

Position of Sensor	Left Side	Right Side
IC2 R - AORTIC	431,5	433,5
IC2 L - PULMONARY	444,0	445,5
IC4 L - TRICUSPID	422,5	424,0
IC5 L - MITRAL	431,5	433,0

Table 52: Auscultation Site B, Patient B: Confidence Intervals for Median of R - S2 Abs Interval (ms)

Position of Sensor	Left Side	Right Side
IC2 R - AORTIC	437,5	439,0
IC2 L - PULMONARY	451,5	454,0
IC4 L - TRICUSPID	433,5	435,0
IC5 L - MITRAL	443,0	444,5

Based on the selection, it can be, on level of certainty 95 % , assured that the medians of R - S2 intervals (R – S2 Abs intervals) are within intervals between the boundaries given in the tables above.

Statistical Hypothesis Testing

This testing determines whether there are statistically significant differences in the duration of R - S2 intervals (R - S2 Abs intervals) obtained from individual chest positions.

- **Parameter tested:** $X_{0.5}$ (Median)
- **Selected test:** Friedman test [51, 52]
- H_0 : $X_{0.5 \text{ interval position AORTIC}} = \dots = X_{0.5 \text{ interval position TRICUSPID}} = X_{0.5 \text{ interval position MITRAL}}$
- H_A : $\neg H_0$
- **Test assumptions:**
 - There is one group of test subjects that are measured on three or more different occasions. ✓
 - The group is a random sample from the population. ✓
 - The dependent variable is at least an ordinal or continuous ✓
- **P - values:**

Table 53: Friedman test: p - values

Tested Intervals	Patient	P - value
R - S2	A	< 0,001
R - S2 Abs	A	< 0,001
R - S2	B	< 0,001
R - S2 Abs	B	< 0,001

- **Results:**

For all tested intervals H_0 was rejected at the 5% significance level. **The differences in the duration of the R - S2 intervals are statistically significant.**

Post Hoc Analysis

From the output of the Friedman test, is known that there are significant differences of R - S2 intervals between tested positions on the chest. To determine, which pairs of positions are different, post hoc analysis is necessary.

Friedman rank sum test with unreplicated blocked data was used for post hoc analysis. [56]

- **P - values:**

Due to the range of p - value tables for individual position pairs, **only pairs where the p - value is greater than or equal to 0,05 are displayed.** Complete tables with p - values are in the Statistics appendix.

Table 54: Patient A, Auscultation site B, R - S2 Abs interval: P - Values from Post Hoc Analysis

Position Pair	P - value
IC2 L PULMONARY - IC4 L TRICUSPID	0,847

Table 55: Patient B, Auscultation site B, R - S2 interval: P - Values from Post Hoc Analysis

Position Pair	P - value
IC2 L AORTIC - IC5 L MITRAL	0,579

- **Results:**

For the most of tested pairs are differences of R - S2 intervals (R - S2 abs intervals) at the 5% significance level statistically important. Duration of R - S2 intervals (R - S2 Abs intervals) is the same only for 2 positions (and methods) mentioned in tables above. But since there is no match between these position pairs for different patients and different detection methods, it can be assumed that the **duration of the R - S2 (R - S2 Abs) interval is dependent on the position of the sensor.**

Conclusion

In this work, nearly 4 hours of multi-channel PCG and ECG recording were measured for 3 patients using two different auscultation sites. This measurement included both normal and degraded data, almost 2 hours of normal data were then completely statistically analysed.

For the detection of S1 and S2, the automatic multiple source heart sound detector was designed. The detector design was based on a proven design using the Shannon energy envelope. In addition to that, the envelope calculation formula was edited and synchronization with the R peak and the T wave of ECG signal was added. The proposed detector allowed 3 different methods of detection S1 (respectively S2), 2 of them were used to calculate the tested intervals (R - S1, R - S2 etc.) that were subsequently processed in statistical analysis. The designed detector enabled to detect heart sounds from all the examined positions (auscultation site A and auscultation site B) on the chest.

Due to the lack of information in the previous research, the spread of the heart sounds on the chest surface was investigated. The aim of the work was to prove whether at the same time the same or at least similar signals could be measured at different positions on the chest. For this purpose, the R - S1 intervals and R - S2 intervals were examined most extensively across the various chest positions. The statistical test results showed that with the chosen method of heart sound detection and selected statistical methods, it can be assumed that there are significant differences between R - S1 intervals obtained from different positions on the chest. This also applies to R - S2 intervals. There are statistically significant differences in time domain for different sensor positioning. For next research, the studies dealing with the analysis of heart sounds and heart sounds detection should take into consideration the position of the sensors.

Determination of optimal localization of the phonocardiograph sensor is very difficult due to the definition. There are many parameters that can be investigated in relation to heart sounds in both the time domain and the frequency domain, similarly, many qualitative and quantitative parameters. The assessment of their optimality depends on what applications and for what purpose the data obtained will be used. Different auscultation findings are expected for different positions of the sensor.

Since PCG signal measurement is not standardized, such as the measurement of ECG signal, it would be interesting to present a design of PCG measurement standardization in a further research paper with respect to the outputs of this thesis. In addition to this thesis, many parameters can be explored in detail to the better understanding of heart sound distribution. An extensive topic could be analysis of the changes in the frequency spectrum of heart sounds for different auscultation areas. Also, an analysis and animation of the S1 sound (respectively S2 sound) energy spread across the chest would be interesting.

References

- [1] Nalos Lukáš, Jitka Švíglerová: Srdeční cyklus. Výukový portál Lékařské fakulty v Plzni [online]. 1.10.2009, Last update 3.1.2013 [cit. 2018-06-27]. ISSN 1804-4409. Available from: <http://mefanet.lfp.cuni.cz/clanky.php?aid=12>
- [2] SOVA, Josef a Josef HŮLA Úvod do elektrokardiografie, fonokardiografie a jiných grafických metod. 2. vyd. Praha: Karlova Univerzita, 1973, 115 s.
- [3] Praktické lékařství [online]. 2007, 2007(3(5) [cit. 2018-06-05]. ISSN 1803-5329. Available from: <https://www.praktickelekarenstvi.cz/pdfs/lek/2007/05/08.pdf>
- [4] MILOŠ ŠTEJFA A SPOLUPRACOVNÍCI. Kardiologie [online]. 3., přeprac. a dopl. vyd. Praha: Grada, 2007 [cit. 2018-06-05]. ISBN 80-247-1385-3. Available from: <https://books.google.fr/books?id=xIRaAgAAQBAJ&lpg=PR1&hl=cs&pg=PA5#v=onepage&q&f=false>
- [5] KANIUSAS, Eugenijus. Biomedical Signals and Sensors II [online]. Berlin, Heidelberg: Springer Berlin Heidelberg, 2015 [cit. 2018-06-15]. Biological and Medical Physics, Biomedical Engineering. ISBN 978-3-662-45105-2.
- [6] PECNÍKOVÁ, Michaela. DETEKCE SRDEČNÍCH OZEV VE FONOKARDIOGRAMU [online]. Brno, 2014 [cit. 2018-06-05]. Available from: https://www.vutbr.cz/www_base/zav_prace_soubor_verejne.php?file_id=86055. BACHELOR'S THESIS. BRNO UNIVERSITY OF TECHNOLOGY.
- [7] ŠPINAR, Jindřich, Ondřej LUDKA a kolektiv. Propedeutika a vyšetřovací metody vnitřních nemocí: 2. Přepřacované a doplněné vydání. Praha: Grada Publishing, 2013. ISBN 9788024783758. Available from: <https://www.grada.cz/propedeutika-a-vysetrovaci-metody-vnitrnich-nemoci-7310/>
- [8] BEJČEK, Ludvík a Jan VACULÍK. Snímače tlaku. AUTOMA [online]. 2011, 2011(1), 20-23 [cit. 2018-03-20]. Available from: http://automa.cz/Aton/FileRepository/pdf_articles/42719.pdf
- [9] Cardiovascular diseases (CVDs). WHO | World Health Organization [online]. Geneva: World Health Organization, 2017 [cit. 2018-06-05]. Available from: [http://www.who.int/en/news-room/fact-sheets/detail/cardiovascular-diseases-\(cvds\)](http://www.who.int/en/news-room/fact-sheets/detail/cardiovascular-diseases-(cvds))
- [10] Auscultation. Physiopedia - universal access to physiotherapy and physical therapy knowledge [online]. [cit. 2018-06-05]. Available from: <https://www.physio-pedia.com/Auscultation>
- [11] MALARVILI, M.B., I. KAMARULAFIZAM, S. HUSSAIN a D. HELMI. Heart sound segmentation algorithm based on instantaneous energy of electrocardiogram. Computers in Cardiology, 2003 [online]. IEEE, 2003, 2003, , 327-330 [cit. 2018-06-05]. DOI:

10.1109/CIC.2003.1291157. ISBN 0-7803-8170-X. Available from: <http://ieeexplore.ieee.org/document/1291157/>

- [12] ABBAS, Abbas K. a Rasha BASSAM. Phonocardiography Signal Processing. Synthesis Lectures on Biomedical Engineering [online]. 2009, 4(1), 1-194 [cit. 2018-06-26]. DOI: 10.2200/S00187ED1V01Y200904BME031. ISSN 1930-0328. Available from: <http://www.morganclaypool.com/doi/abs/10.2200/S00187ED1V01Y200904BME031>
- [13] ARNOTT, P.J., G.W. PFEIFFER a M.E. TAVEL. Spectral analysis of heart sounds: Relationships between some physical characteristics and frequency spectra of first and second heart sounds in normals and hypertensives. Journal of Biomedical Engineering [online]. 1984, 6(2), 121-128 [cit. 2018-06-05]. DOI: 10.1016/0141-5425(84)90054-2. ISSN 01415425. Available from: <http://linkinghub.elsevier.com/retrieve/pii/0141542584900542>
- [14] EL-SEGAIER, M., O. LILJA, S. LUKKARINEN, L. SÖRNMO, R. SEPPONEN a E. PESONEN. Computer-Based Detection and Analysis of Heart Sound and Murmur. Annals of Biomedical Engineering [online]. 2005, 33(7), 937-942 [cit. 2018-06-05]. DOI: 10.1007/s10439-005-4053-3. ISSN 0090-6964. Available from: <http://link.springer.com/10.1007/s10439-005-4053-3>
- [15] LIANG, H., S. LUKKARINEN a I. HARTIMO. Heart sound segmentation algorithm based on heart sound envelopogram. Computers in Cardiology 1997 [online]. IEEE, 1997, , 105-108 [cit. 2018-06-05]. DOI: 10.1109/CIC.1997.647841. ISBN 0-7803-4445-6. Available from: <http://ieeexplore.ieee.org/document/647841/>
- [16] WOOD, J.C. a D.T. BARRY. Time-frequency analysis of the first heart sound. IEEE Engineering in Medicine and Biology Magazine [online]. 14(2), 144-151 [cit. 2018-06-05]. DOI: 10.1109/51.376751. ISSN 07395175. Available from: <http://ieeexplore.ieee.org/document/376751/>
- [17] RAJAN, S., R. DORAISWAMI, R. STEVENSON a R. WATROUS. Wavelet based bank of correlators approach for phonocardiogram signal classification. Proceedings of the IEEE-SP International Symposium on Time-Frequency and Time-Scale Analysis (Cat. No.98TH8380) [online]. IEEE, 1998, , 77-80 [cit. 2018-06-05]. DOI: 10.1109/TFSA.1998.721365. ISBN 0-7803-5073-1. Available from: <http://ieeexplore.ieee.org/document/721365/>
- [18] GILL, D., N. GAVRIELI a N. INTRATOR. Detection and identification of heart sounds using homomorphic envelopogram and self-organizing probabilistic model. Computers in Cardiology, 2005 [online]. IEEE, 2005, 2005, , 957-960 [cit. 2018-06-05]. DOI: 10.1109/CIC.2005.1588267. ISBN 0-7803-9337-6. Available from: <http://ieeexplore.ieee.org/document/1588267/>

- [19] CHAUHAN, Sunita, Ping WANG, Chu SING LIM a V. ANANTHARAMAN. A computer-aided MFCC-based HMM system for automatic auscultation. *Computers in Biology and Medicine* [online]. 2008, 38(2), 221-233 [cit. 2018-06-05]. DOI: 10.1016/j.compbio.2007.10.006. ISSN 00104825. Available from: <http://linkinghub.elsevier.com/retrieve/pii/S0010482507001722>
- [20] GAMERO, L.G. a R. WATROUS. Detection of the first and second heart sound using probabilistic models. *Proceedings of the 25th Annual International Conference of the IEEE Engineering in Medicine and Biology Society (IEEE Cat. No.03CH37439)* [online]. IEEE, 2003, , 2877-2880 [cit. 2018-06-05]. DOI: 10.1109/IEMBS.2003.1280519. ISBN 0-7803-7789-3. Available from: <http://ieeexplore.ieee.org/document/1280519/>
- [21] OSKIPER, T. a R. WATROUS. Detection of the first heart sound using a time-delay neural network. *Computers in Cardiology* [online]. IEEE, 2002, 2002(29), 537-540 [cit. 2018-06-05]. DOI: 10.1109/CIC.2002.1166828. ISBN 0-7803-7735-4. Available from: <http://ieeexplore.ieee.org/document/1166828/>
- [22] SHARMA, Praveen Kumar; SAHA, Sourav; KUMARI, Saraswati. Study and design of a Shannon-energy-envelope based phonocardiogram peak spacing analysis for estimating arrhythmic heart-beat. *International Journal of Scientific and Research Publications*, 2014, 4.9. Available from: <http://citeseerx.ist.psu.edu/viewdoc/download?doi=10.1.1.656.1128&rep=rep1&type=pdf#page=134>
- [23] DOKUR, Zümray a Tamer ÖLMEZ. Heart sound classification using wavelet transform and incremental self-organizing map. *Digital Signal Processing* [online]. 2008, 18(6), 951-959 [cit. 2018-06-05]. DOI: 10.1016/j.dsp.2008.06.001. ISSN 10512004. Available from: <http://linkinghub.elsevier.com/retrieve/pii/S1051200408000961>
- [24] WANG, Xinpei, Yuanyang LI, Churan SUN a Changchun LIU. Detection of the First and Second Heart Sound Using Heart Sound Energy. In: *2009 2nd International Conference on Biomedical Engineering and Informatics* [online]. IEEE, 2009, 2009, s. 1-4 [cit. 2018-06-07]. DOI: 10.1109/BMEI.2009.5305640. ISBN 978-1-4244-4132-7. Available from: <http://ieeexplore.ieee.org/document/5305640/>
- [25] DJEBBARI, A. a F. BEREKSI REGUIG. Short-time Fourier transform analysis of the phonocardiogram signal. *ICECS 2000. 7th IEEE International Conference on Electronics, Circuits and Systems (Cat. No.00EX445)* [online]. IEEE, 2000, 2000, 844-847 [cit. 2018-06-06]. DOI: 10.1109/ICECS.2000.913008. ISBN 0-7803-6542-9. Available from: <http://ieeexplore.ieee.org/document/913008/>
- [26] JUNG JUN LEE, SANG MIN LEE, IN YOUNG KIM, HONG KI MIN a SEUNG HONG HONG. Comparison between short time Fourier and wavelet transform for feature extraction of heart sound. *Proceedings of IEEE. IEEE Region 10 Conference. TENCON 99.*

- 'Multimedia Technology for Asia-Pacific Information Infrastructure' (Cat. No.99CH37030) [online]. IEEE, 1999, , 1547-1550 [cit. 2018-06-06]. DOI: 10.1109/TENCON.1999.818731. ISBN 0-7803-5739-6. Available from: <http://ieeexplore.ieee.org/document/818731/>
- [27] SCHMIDT, S E, C HOLST-HANSEN, C GRAFF, E TOFT a J J STRUIJK. Segmentation of heart sound recordings by a duration-dependent hidden Markov model. *Physiological Measurement* [online]. 2010, 31(4), 513-529 [cit. 2018-06-07]. DOI: 10.1088/0967-3334/31/4/004. ISSN 0967-3334. Available from: <http://stacks.iop.org/0967-3334/31/i=4/a=004?key=crossref.678dca4d8aec1b82b003add452871614>
- [28] CHOI, S a Z JIANG. Comparison of envelope extraction algorithms for cardiac sound signal segmentation. *Expert Systems with Applications* [online]. 2008, 34(2), 1056-1069 [cit. 2018-06-07]. DOI: 10.1016/j.eswa.2006.12.015. ISSN 09574174. Available from: <http://linkinghub.elsevier.com/retrieve/pii/S0957417406003927>
- [29] SEPEHRI, Amir A., Arash GHAREHBAGHI, Thierry DUTOIT, Armen KOCHARIAN a A. KIANI. A novel method for pediatric heart sound segmentation without using the ECG. *Computer Methods and Programs in Biomedicine* [online]. 2010, 99(1), 43-48 [cit. 2018-06-07]. DOI: 10.1016/j.cmpb.2009.10.006. ISSN 01692607. Available from: <http://linkinghub.elsevier.com/retrieve/pii/S0169260709002909>
- [30] GUPTA, Cota Navin, Ramaswamy PALANIAPPAN, Sundaram SWAMINATHAN a Shankar M. KRISHNAN. Neural network classification of homomorphic segmented heart sounds. *Applied Soft Computing* [online]. 2007, 7(1), 286-297 [cit. 2018-06-07]. DOI: 10.1016/j.asoc.2005.06.006. ISSN 15684946. Available from: <http://linkinghub.elsevier.com/retrieve/pii/S1568494605000694>
- [31] CHUNG-HSIEN WU, CHING-WEN LO a JHING-FA WANG. Computer-aided analysis and classification of heart sounds based on neural networks and time analysis. In: 1995 International Conference on Acoustics, Speech, and Signal Processing [online]. IEEE, 1995, s. 3455-3458 [cit. 2018-06-07]. DOI: 10.1109/ICASSP.1995.479729. ISBN 0-7803-2431-5. Available from: <http://ieeexplore.ieee.org/document/479729/>
- [32] CHAUDHURI, Ananddeep a T. JAYANTHI. Effective S1 S2 detection system with beat track method. In: 2016 International Conference on Wireless Communications, Signal Processing and Networking (WiSPNET) [online]. IEEE, 2016, 2016, s. 714-718 [cit. 2018-06-11]. DOI: 10.1109/WiSPNET.2016.7566226. ISBN 978-1-4673-9338-6. Available from: <http://ieeexplore.ieee.org/document/7566226/>
- [33] CHOI, S a Z JIANG. Comparison of envelope extraction algorithms for cardiac sound signal segmentation. *Expert Systems with Applications* [online]. 2008, 34(2), 1056-1069 [cit. 2018-06-11]. DOI: 10.1016/j.eswa.2006.12.015. ISSN 09574174. Available from: <http://linkinghub.elsevier.com/retrieve/pii/S0957417406003927>

- [34] HAMZA CHERIF, Lotfi. SEGMENTATION OF HEART SOUNDS AND HEART MURMURS. Journal of Mechanics in Medicine and Biology [online]. 2008, 8(4), 549-559 [cit. 2018-06-12]. Available from: https://www.researchgate.net/publication/292411385_SEGMENTATION_OF_HEART_SOUNDS_AND_HEART_MURMURS?_sg=ao7nwAOWMdExjLjp-9i5pCbJDBkxtBMMO_k-WmrZjlblbl7C01jZZc11bHfGMLxX420CjWp6Kg
- [35] SHARMA, L. N. Multiscale analysis of heart sound for segmentation using multiscale Hilbert envelope. In: 2015 13th International Conference on ICT and Knowledge Engineering (ICT & Knowledge Engineering 2015) [online]. IEEE, 2015, 2015, s. 33-37 [cit. 2018-06-14]. DOI: 10.1109/ICTKE.2015.7368467. ISBN 978-1-4673-9189-4. Available from: <http://ieeexplore.ieee.org/document/7368467/>
- [36] PowerLab Data with integrity. ADInstruments [online]. 2018 [cit. 2018-06-27]. Available from: <https://www.adinstruments.com/products/powerlab>
- [37] PAN, Jiapu a Willis J. TOMPKINS. A Real-Time QRS Detection Algorithm. IEEE Transactions on Biomedical Engineering [online]. 1985, BME-32(3), 230-236 [cit. 2018-06-12]. DOI: 10.1109/TBME.1985.325532. ISSN 0018-9294. Available from: <http://ieeexplore.ieee.org/document/4122029/>
- [38] SEDGHAMIZ, Hooman. Matlab Implementation of Pan Tompkins ECG QRS detector [online]. 2014 [cit. 2018-06-12]. DOI: 10.13140/RG.2.2.14202.59841. Available from: https://www.researchgate.net/publication/313673153_Matlab_Implementation_of_Pan_Tompkins_ECG_QRS_detector
- [39] ELGENDI, Mohamed, Bjoern ESKOFIER a Derek ABBOTT. Fast T Wave Detection Calibrated by Clinical Knowledge with Annotation of P and T Waves. Sensors [online]. 2015, 15(7), 17693-17714 [cit. 2018-06-13]. DOI: 10.3390/s150717693. ISSN 1424-8220. Available from: <http://www.mdpi.com/1424-8220/15/7/17693>
- [40] SAHAMBI, J.S., S.N. TANDON a R.K.P. BHATT. Using wavelet transforms for ECG characterization. An on-line digital signal processing system. IEEE Engineering in Medicine and Biology Magazine [online]. 16(1), 77-83 [cit. 2018-06-13]. DOI: 10.1109/51.566158. ISSN 07395175. Available from: <http://ieeexplore.ieee.org/document/566158/>
- [41] ISSA, Ziad F., John M. MILLER a Douglas P. ZIPES. Intraventricular Conduction Abnormalities. Clinical Arrhythmology and Electrophysiology: A Companion to Braunwald's Heart Disease [online]. Elsevier, 2012, 2012, s. 194-211 [cit. 2018-06-13]. DOI: 10.1016/B978-1-4557-1274-8.00010-5. ISBN 9781455712748. Available from: <http://linkinghub.elsevier.com/retrieve/pii/B9781455712748000105>

- [42] SURAWICZ, Borys a TIMOTHY K. KNILANS. Chou's electrocardiography in clinical practice adult and pediatric. 6th ed. Philadelphia, PA: Saunders/Elsevier, 2008. ISBN 1437711022.
- [43] GROSS, Desiderio. The duration of the T wave and its relation to the cardiac rate in healthy adults. American Heart Journal [online]. 1954, 47(4), 514-519 [cit. 2018-06-13]. DOI: 10.1016/0002-8703(54)90233-1. ISSN 00028703. Available from: <http://linkinghub.elsevier.com/retrieve/pii/0002870354902331>
- [44] FREQUENCY BANDS EFFECTS ON QRS DETECTION. In: Proceedings of the Third International Conference on Bio-inspired Systems and Signal Processing [online]. SciTePress - Science and and Technology Publications, 2010, 2010, s. 428-431 [cit. 2018-06-14]. DOI: 10.5220/0002742704280431. ISBN 978-989-674-018-4. Available from: <http://www.scitepress.org/DigitalLibrary/Link.aspx?doi=10.5220/0002742704280431>
- [45] WALKER, H. Kenneth, W. Dallas HALL a J. Willis HURST. Clinical methods: the history, physical, and laboratory examinations. 3rd ed. Boston: Butterworths, c1990. ISBN 978-0409900774.
- [46] LUISADA, Aldo A.; MENDOZA, Felipe; ALIMURUNG, Mariano M. The duration of normal heart sounds. British heart journal, 1949, 11.1: 41.
- [47] KANIUSAS, Eugenijus. Biomedical Signals and Sensors II [online]. Berlin, Heidelberg: Springer Berlin Heidelberg, 2015 [cit. 2018-06-15]. Biological and Medical Physics, Biomedical Engineering. ISBN 978-3-662-45105-2.
- [48] BAYKAL, A., Y. ZIYA IDER a H. KOYMEN. Distribution of aortic mechanical prosthetic valve closure sound model parameters on the surface of the chest. IEEE Transactions on Biomedical Engineering [online]. 42(4), 358-370 [cit. 2018-06-25]. DOI: 10.1109/10.376129. ISSN 00189294. Available from: <http://ieeexplore.ieee.org/document/376129/>
- [49] MALARVILI, M.B., I. KAMARULAFIZAM, S. HUSSAIN a D. HELMI. Heart sound segmentation algorithm based on instantaneous energy of electrocardiogram. Computers in Cardiology, 2003 [online]. IEEE, 2003, 2003, , 327-330 [cit. 2018-06-05]. DOI: 10.1109/CIC.2003.1291157. ISBN 0-7803-8170-X. Available from: <http://ieeexplore.ieee.org/document/1291157/>
- [50] Shapiro-Wilk Normality Test. Statistical Data Analysis [online]. [cit. 2019-04-20]. Available from: <https://stat.ethz.ch/R-manual/R-devel/library/stats/html/shapiro.test.html>
- [51] LITSCHMANNOVÁ, Martina. Úvod do statistiky [online]. Ostrava: VŠB – TU Ostrava, Fakulta elektrotechniky a informatiky, 2016 [cit. 2019-04-20]. Available from: http://mi21.vsb.cz/sites/mi21.vsb.cz/files/unit/uvod_do_statistiky.pdf

- [52] Friedman Rank Sum Test. Statistical Data Analysis [online]. Zurich [cit. 2019-04-20]. Available from: <https://stat.ethz.ch/R-manual/R-patched/library/stats/html/friedman.test.html>
- [53] Wilcoxon Rank Sum and Signed Rank Tests. Statistical Data Analysis [online]. Zurich [cit. 2019-04-20]. Available from: <https://stat.ethz.ch/R-manual/R-patched/library/stats/html/wilcox.test.html>
- [54] Kruskal-Wallis Rank Sum Test. Statistical Data Analysis [online]. Zurich [cit. 2019-04-20]. Available from: <https://stat.ethz.ch/R-manual/R-patched/library/stats/html/kruskal.test.html>
- [55] DINNO, Alexis. Dunn's Test of Multiple Comparisons Using Rank Sums. The Comprehensive R Archive Network [online]. 2017 [cit. 2019-04-21]. Available from: <https://cran.r-project.org/web/packages/dunn.test/dunn.test.pdf>
- [56] Friedman Rank Sum Test. Statistical Data Analysis [online]. Zurich [cit. 2019-04-20]. Available from: <https://stat.ethz.ch/R-manual/R-patched/library/stats/html/friedman.test.html>

List of Appendices

CD attachment

Directory structure of the CD:

- Statistics
- Heart Sound Detector